Chem Soc Rev

Graphene/Nucleic Acids Nanobiointerface

Journal:	*Chemical Society Reviews*
Manuscript ID:	CS-SYN-12-2014-000519.R2
Article Type:	Review Article
Date Submitted by the Author:	11-Jun-2015
Complete List of Authors:	Li, Jinghong; Tsinghua Univ, Chemistry Wang, Ying; Tongji University, State Key Laboratory of Pollution Control and Resource Reuse Study Tang, Tonghua; tsinghua Univ,

Graphene/Nucleic Acid Nanobiointerface

Longhua Tang [b‡], Ying Wang [c‡], and Jinghong Li [a]*

[a] *Department of Chemistry, Beijing Key Laboratory for Microanalytical Methods and Instrumentation, Tsinghua University, Beijing 100084, China*

[b] *State Key Laboratory of Modem Optical Instrumentation, Department of Optical Engineering, Zhejiang University, Hangzhou 310027, China*

[c] *Department of Chemistry, Shanghai Key Laboratory of Chemical Assessment and Sustainability, Tongji University, Shanghai, 200092, China*

‡ Dr. L. H. Tang and Dr. Y. Wang contributed equally to this work.
* Corresponding author, Email: jhli@mail.tsinghua.edu.cn

Abstract

The combination of nanomaterials with biomolecules yields functional nanostructured biointerfaces with synergistic properties and functions. Owing to a unique combination of its crystallographic and electronic structure, graphene and its derivatives exhibit several superior and typical properties, which has emerged as an attractive candidate for fabrication of the novel nanobiointerface with kinds of unique applications. As known, nucleic acids are stable and ease to handle the modification, and can recognize a wide range of targets with high selectivity, specificity, and affinity. The integration of nucleic acids with graphene-based materials has been substantially advanced in the past few years, which achieved amazing properties and functions, thereby exhibiting attractive potential applications in biosensing, diagnostics, drug screening and biomedicine. Herein, this review addresses the recent progress on design and fabrication of graphene/nucleic acid nanostructured biointerface, fundamental understanding of their interfacial properties, as well as the various nanobiotechnological applications. To begin with, we summarize the basic features of the graphene and nucleic acid-based nanobiointerface, especially the interfacial interaction mechanism and the resulted biological effects. Then, fabrication and characterization methodology of graphene and nucleic acids-based nanobiointerface are discussed. Next, particular emphasis is directed to the exploration of their biosensing and biomedical applications, including small molecule detection, protein and DNA sensing/sequencing, as well as gene delivery and therapy. Finally, some significant prospects, further opportunities and challenges in this emerging field are also suggested.

Keywords：Graphene; Nucleic Acid; Interface; Biosensor; Drug Delivery; Cell Imaging

1. Introduction

Nanobiotechnologies are being applied to many fields of science and engineering, which hold one of the greatest significant promises.[1-9] This highly interdisciplinary field focuses on several important areas of research, including biological inspired nanomaterials synthesis, nanomaterials-mediated regulate biological processes, biocompatible nanostructures fabrication for the use in both biology and medicine, and so on.[10] Advances in this field offer novel and potentially useful approaches for building functional structures, such as energy generation, conversion and storage materials, optical devices, and new detection and therapeutic tools.[4, 5, 9-12] Although the field is still embryonic, major achievements have been made.

As one subfield of nanobiotechnology, how the biosystem reacts to nanomaterials and how the nanostructured biointerface works, are drawing a great attention. Indeed, the exploration and fabrication of nanobiointerface are emerging at the intersection of material sciences, and molecular biotechnology, which is closely associated with both the physical and chemical properties of nanomaterials, as well as to the various aspects of biology.[4, 5, 13] With the rapid advance in nanoscience and nanotechnology, a wide range of nanostructures have been introduced to nanobiotechnology. The unique properties of nanostructures facilitate the fabrication of functional nanostructured biointerfaces. Moreover, by adjusting the biological activity of the biointerface appropriately, these nanostructured biointerfaces would exhibit the capability for characteristic bio/nano applications. Considering its multidisciplinary nature, the nanobiointerface is to study the interfacial interactions between the nanostructured

materials interaction with biological systems, and further on a higher level between the so-called exact sciences (e. g., physics, chemistry) and the life sciences.

Over the past three decades, biotechnology and material science have developed into the powerful disciplines. Since the 1990's, studies have originated on interfacing nanomaterials with biocomponents, with the goal of monitoring biomolecules or bio-related phenomena. In 1996, Mirkin's group[14] and Alivisatos's group[15] experimentally demonstrated not only that DNA could be used for the organization of nanostructures, but also that nanoparticles were highly sensitive to the DNA hybridization events.[16,17] As successful synthesis of crystalline, size-selected, and epitaxially capped semiconductor quantum dots (QDs) early in the 1990s, QDs conjugated with antibodies were used for targeting with specific biomolecules in cells and also for effective intracellular imaging.[18-21] Lately, bioconjugated magnetic nanoparticles were found with the capability for sophisticated imaging and targeted destruction of cancer cells.[22-24] Almost simultaneously, carbon nanotubes were discovered,[25] and several versatile semiconductor nanowires were grown.[26-28] As their extreme aspect ratio and sensitivity to charge-transfer interaction, nanotubes and nanowires were revealed as the sensitive sensing platforms for the detection of biomolecules.[29-31] Research in the current decade has led to seeking sophisticated tools for tailoring particles to specific problems in sensing, imaging, drug delivery and therapy. Moreover, various bio/nano systems were proposed with applying zero-dimensional (0D) and one-dimensional (1D) nanomaterials (semiconducting nanoparticles, silicon nanowires, *etc.*), which led to the development of valuable tools

and devices for biosensing, diagnostics and biomedicine.[29-32]

Since its discovery in 2004, [33] graphene has generated great interest and leading to the rapid development of two-dimensional (2D) nanotechnology. Owing to a unique combination of its crystallographic and electronic structure, graphene and its derivatives exhibit several superior physical, chemical and mechanical properties,[34-39] which has emerged as an attractive candidate for the fabrication of the novel nanobiointerface with kinds of unique applications.[12, 35, 40-44] In particular, the coupling of nucleic acids with graphene-based materials has substantially attracted much more attention in the past several years.[42-46] As known, nucleic acids are stable and ease to handle the modification, and can recognize a wide range of targets with high selectivity, specificity, and affinity.[47-49] Therefore, nucleic acids-interfacial graphene would achieve improved properties and functions, such as good biocompatibility and biomolecular recognition capabilities, thereby exhibiting attractive potential for further applications, such as biosensing, diagnostics, drug screening and efficient drug delivery.

With the advent of the rapidly growing field of exploration and fabrication of the nano/bio interfaces between nanomaterials and biocomponents, the integration of nucleic acids with graphene has been substantially advanced. This review addresses recent advances in the fabrication, exploration, and applications of nucleic acids-functionalized graphene biointerfaces. Discussions about the interfacial fundamental and properties are presented and schematically illustrated in **Scheme 1**. To begin with, we summarize the fundamental and methodology of the

graphene-nucleic acid interface, and the related biological effect. Sequentially, the analytical approaches of graphene and nucleic acids-based functional nanostructured biointerfaces are discussed, emphatically on the techniques such as fluorescence resonance energy transfer (FRET), electrochemistry, field-effect transistor (FET) and nanopore-based analysis. Next, particular emphasis is directed to the exploration of applications in biotechnology, including small molecule detection, protein and immuno-biotechnology, as well as the DNA sensing/sequencing. Furthermore, gene delivery and therapy, drug delivery and biomedical potentials by utilizing graphene and nucleic acid-based nanobiointerface are summarized, showing its amazing prospects of this unique inorganic-organic complex. Finally, some significant prospects and further developments in this exciting interdisciplinary field are also suggested.

2. Graphene and Nucleic Acid-based Nanobiointerface

2.1 Brief Introduction to Graphene Physics and Chemistry

Graphene is a 2D carbon material, constituting a single- or few-layered sheet of sp^2-bonded carbon atoms, which are closely packed in a honeycomb lattice structure.[34-39] Since it is considered as the basic building block of the other graphitic materials in the different dimensions, graphene are also considered as “the mother of all graphitic forms” [38] For example, graphene can be wrapped up into 0D fullerene, rolled up into 1D nanotube or several graphene layers stacked into 3D graphite. Experiments and/or theories have revealed that graphene exhibits a quantum Hall effect at room temperature, ambipolar electric field effect along with ballistic conduction of charge carriers, high room-temperature electron mobility, tunable

optical properties, a specific surface area, high elasticity and thermal conductivity.[50-59] All these properties distinguish graphene from ordinary materials, and make graphene excite the scientific community especially in the areas of materials, physics, and chemistry.[50-59] To develop a integrate understanding of its nature and realize the full potential of graphene, extensive investigations have proceeded in various directions.

Although expected to be a single-layer or few-layer carbon sheet, the term graphene has been used loosely in the literature, which represents not only pristine graphene but also many other derivatives with some similar characteristics, all of which we include under the umbrella of graphene.[50-52] In this review, most of referred graphene-related derivatives is graphene oxide (GO), which is obtained by deep oxidation of graphite and subsequent exfoliation of the resulting graphite oxide, which may contain a high proportion of oxygen, in some cases higher than that of carbon. Due to the ease of preparation in large quantities from available graphite, GO has been one of the preferred graphene derivatives as catalysts, sensing platform and other useful substrate. [53-56] A comprehensive description of graphene properties is not provided as they can be found in various recent publications.[57-59]

To date, several strategies have since been developed for the synthesis of graphene, including the top-down (*e.g.* micro-mechanical cleavage) methods and bottom-up (*e.g.* chemical vapor deposition, CVD) methods.[50,60,71] For instance, graphene has been obtained by epitaxial growth on insulating substrates such as SiC and SiO_2, and on metal substrates such as Ir (111) and Ni (111).[58-61] CVD and chemical exfoliation, thermal oxidation of graphite have made the preparation of large-area graphene

feasible.[56, 62] Of these techniques developed to produce graphene, chemical methods are effective for producing graphene sheets from various precursors on a large scale at low cost, which enables technical applications in a variety of fields. Particularity, one of the most used methods for mass production is chemical synthesis process from graphite by oxidation and subsequent reduction.

The chemistry of graphene has been extensively investigated in the past few years.[37,45] Intensive efforts have been devoted to fabricate large-area graphene with minimal defects for various applications; whereas for biosensing and/or biomedical applications of graphene in physiological environments, proper surface functionalization on graphene is demanded to render high water solubility and biocompatibilitys. From the chemical modification perspective, graphene can be functionalized by both covalent and non-covalent strategies.[53,67] Covalent chemistry, such as 1,3-dipolar cycloadition and carbodiimide chemistry N-(3-dimethylaminopropyl)-N′-ethylcarbodiimide hydrochloride (EDC) coupling chemistry, has been developed to modify graphene (including CVD-grown or exfoliated pristine graphene).[68] While, the non-covalent chemistry is particularly interesting for biosensing, drug delivery, as many aromatic molecules can be physically adsorbed on the polyaromatic graphene surface by π-π stacking [69-75] Due to the presence of aromatic domains and multiple oxygen functional groups, GO has more potential applications in biological system,[44,53-56] which is ease to handle via both covalent and non-covalent functionalization chemistry.[76-79]

Along with advancement of graphene-centered science and biotechnology, various nano/bio interfaces have been realized in the areas of bioanalytical chemistry, molecular medicine and nanobiotechnologies. Especially, graphene has been widely employed as a substrate to be interfaced with various biomolecules and cells, including proteins and nucleic acids.

2.2. Nucleic Acids

As known, nucleic acids are polymeric biological molecules, including DNA (deoxyribonucleic acid) and RNA (ribonucleic acid), which are made from monomers known as nucleotides. Each nucleotide has three components of a five-carbon sugar, a phosphate group, and a nitrogenous base. If the sugar is deoxyribose, the polymer is DNA; if the sugar is ribose, the polymer is RNA. Nucleotides strung together in a specific sequence are the mechanism for storing and transmitting hereditary or genetic, information *via* protein synthesis. Research on nucleic acid has always been inherently interdisciplinary, encompassing biology, chemistry, and medicine.[80] In recent years, series of called functional nucleic acids (FNAs), including natural FNAs (*e.g.* Ribozymes and Riboswitches) and artificial FNAs (*e.g.* aptamers, DNAzyme, and aptazymes), are produced. by a combinatorial method called *in vitro* selection or systematic evolution of ligands by exponential enrichment (SELEX), whose functions are beyond the conventional genetic roles of nucleic acids.[81-83] For instance, aptamer, the specific DNA or RNA binding with high affinity and specificity to targets, is pretty useful in biotechnological and therapeutic applications, as they offer molecular recognition properties and other advantages over antibodies such as stability and

higher binding affinity.[82,84,85] One other class of important synthetic oligonucleotides, called molecular beacons (MBs), are hairpin shaped molecules with an internally quenched fluorophore that can report the presence of specific nucleic acids in homogenous solutions.[86,] Moreover, both of DNA and RNA molecule possess remarkable self-assembly features and programmable biorecognition capability. Therefore, combination of the extraordinary properties of nanomaterials with the FNA units can result in a robust nanomaterials-nucleic acids biointerface, which should have fundamental significance and practical importance in many fields.[29, 32, 72, 87-92]

2.3 Graphene Biointerfacing with Nucleic Acid

The interplay of graphene with nano/micrometer-scale bio-components (DNA, proteins, bacteria and other cells, *etc.*) has been profoundly investigated, and fascinated practical applications in material science, molecular recognition, and biomedical imaging. To date, the theoretical studies for the adsorption mechanism between graphene and nucleic acids have been carried out, to explore the binding mechanism and the relative binding strength of four DNA nucleobases [guanine (G), adenine (A), thymine (T), and cytosine (C)].[93- 102]

Gowtham *et al.*[101] used density functional theory (DFT) formalism with plane-wave pseudopotential considering periodic lattice of graphene-nucleobase complexes, finding significant differences between interaction strengths when a nucleobase is physisorbed on graphene. The analysis of binding energies illustrated that the base molecule polarizabilities would effectively determine the nucleobase-graphene interaction strength. Varghese *et al.* optimized structures of graphene-nucleobase

complexes using Hartree-Fock method,[93] whereas Sastry and co-workers [99] studied interaction of graphene with the nucleobases using dispersion-corrected DFT based approach, finding that the binding energy depends on curvature of the molecule. Bhattacharyya and co-workers have carried out detailed quantum chemical calculations of complexes of graphene nanosheets and the nucleobases using dispersion corrected DFT.[94] Basically, these planar nucleobase-graphene model systems simplified the complexity of DNA structure adsorbed on graphene, thereby to provide a possibility for direct experimental characterization of the molecular interactions with graphene. According to previous DFT calculations within the local density approximation (LDA),[101] the binding energy of the nucleobases on graphene varies in the order of G > A ≈ T ≈ C. If calculation with the more accurate second-order Møller-Plesset perturbation theory and the DFT methods including *van der* Waals interactions,[99, 123] the binding energy strengths of nucleobases with graphene was suggested to be the ordering of G > A > T > C, which was consistent with the single solute adsorption isotherm study at the graphite-water interface.[104]

In addition, the interaction between nucleic acid and graphene has also been experimentally studied, partially thanks to the significant improvement of high-resolution measurement methods.[46, 105-111] It is demonstrated that the large 2D graphene or GO can bind single-stranded DNA (ssDNA) *via* hydrophobic and π-π stacking interactions between the ring structures in the nucleobases and the hexagonal cells of graphene. Patil *et al.*[112] reported the use of DNA in the preparation of stable aqueous suspensions of graphene and proposed a DNA and graphene interaction

mechanism (surface binding model) which was similar to that of carbon nanotubes.[113] It was demonstrated that DNA electrostatically interacted with graphene basal planes and ssDNA showed much stronger affinity towards graphene than double-stranded (ds) DNA. As Lu and coworker reported, GO could bind and quench dye-labeled ssDNA probes, while it has less affinity toward dsDNA or secondary and tertiary structured ssDNA.[110] Fan and co-workers further carried out the molecular dynamics (MD) simulation to investigate the observed large difference in binding affinity of ss- and ds-DNA with GO.[113] Wu and co-workers studied the adsorption and desorption of DNA oligonucleotides on GO as a function of salt concentration and DNA length.[105] They found that shorter DNAs were adsorbed more rapidly and bind more tightly to graphene, and the adsorption was favored by a lower pH and a higher ionic strength. Yi et *al.* designed an aptamer-two-photon dye/GO-based fluorescent nanosensing conjugate for molecular probing the binding affinity of the aptamer to the target in biological fluids, living cells, and zebrafish.[106] On the other hand, Yang and coworkers investigated the binding ability and stability of ssRNA on GO, finding that ssRNA could bind strongly to the GO surface and be effectively protected from enzymatic cleavage.[108] On the basis of above findings, ssDNA/ssRNA-graphene complexes have been used for the detection of a variety of analytes.

It is known that the binding between ssDNA/ssRNA and graphene is ascribed to the π-π stacking interactions between them, however, there are still controversies about the driving force for the interactions between ds-DNA/RNA and graphene.[115-117] Several studies suggested that the hydrophilic external surface of dsDNA/dsRNA

could prevent favorable interaction with the hydrophobic graphene surface.[114] Whereas, several reports indicated the hydrogen bonding or *van der* Waals attractive forces between DNA and graphene would be sufficient to render the DNA adsorbed on the graphene. For examples, Lei *et al.* reported that dsDNA could bind to GO, forming dsDNA/GO complex in the presence of a high concentration of salts.[117] Zhao *et al.* used molecular dynamics simulations to study the interaction of dsDNA segments with the surfaces of graphene in aqueous solution,[118] finding that DNA duplex could self-assemble on the graphene surface by the π-stacking interactions between the ending base pairs of DNA and graphene. The simulations, however, did not consider the counter ions, or charges on the graphene or its derivatives like GO, so that electrostatic force and hydrogen bonding were not considered. In order to clarify these controversies, we systematically investigated the interaction between DNA and GO with series of experiments, finding that DNA duplexes interacted with GO may be facilitated by partial deformation of the DNA double helix.[115] In combination with fluorescence and melting results, the primary driving force was suggested to be π-stacking interactions between the ending base pairs of DNA and the carbon rings. On the other hand, we supposed that the binding affinity of dsDNA to GO may also be enhanced by hydrogen-bond formation between oxygenous groups of GO and DNA bases. These results coincide well with previous molecular dynamics calculations.[118]

3. Biological Effects of Graphene/Nucleic Acid Interface

Nanomaterials show special biological effects due to their unique structures and properties when interacting with biocomponents.[119,121] For examples, protective ability of nanomaterials with nucleic acids has been reported for silica nanoparticles,[122] silica nanotubes,[123] gold nanoparticles (GNPs),[124] and carbon nanotubes (CNTs). [125-128] Recently, numerous works demonstrated that nucleic acids binding on graphene or its derivative could be effectively protected from nuclease digestion. Tang *et al.* reported the protection behaviors of GO to ssDNA, showing that ssDNA adsorbed on GO surfaces can be effectively protected from enzymatic cleavage by deoxyribonuclease (DNAse I, a common enzyme that promotes DNA degradation)[129] Lately, other groups also observed similar results.[110, 119, 121, 130-136] Furthermore, we and other groups investigated the biological behaviors of DNA duplex assembled on graphene surface, such as specific enzyme cleavage effect. [115, 116, 117,133] It was demonstrated that the protective effect of ssDNA and dsDNA could be freely tuned by adjusting the salt concentration.[117] At low salt concentrations, the adsorbed ssDNA on GO was protected from nuclease digestion, while the desorbed dsDNA could be digested. However, when the salt concentration was increased, dsDNA could be adsorbed on the GO surface and be protected from nuclease digestion, showing that dsDNA on GO could be effectively cleaved by DNA enzyme I and restriction endonucleases as EcoR I, while being highly resistant to the degradation by Exo III.[115] As reported, the binding affinity of nucleic acid on GO was found to be affected by experimental conditions.[64, 77, 134, 136] Therefore, in order to establish an ideal GO-protected nucleic acid system, certain critical experimental

conditions, such as buffer solution, incubation time, concentration of nucleic acid and nuclease, were needed to be optimized.

Although it is still elusive for the mechanisms of the protection property of graphene on nucleic acid, there are some common senses as proposed in some reports.[149,151, 121] First, the interaction between nucleic acid and graphene may cause a conformational change of the nucleic acid, rendering its unrecognizable by enzyme binding pockets and protected from cleavage. Second, the change of local ion concentration induced by graphene inhibited enzyme activity. This point was also presented to interpret the protective properties of silica and GNPs.[122-124] Third, the most popular perspective is steric hindrance, which prevents nuclease from approaching the nucleic acids to initiate enzymatic hydrolysis. Likewise, nucleic acid adsorption on graphene can result in steric hindrance, change in local ion concentration, or change in probe conformation, thereby protecting nucleic acid from nuclease digestion.[115]

4. Analysis Methods for Graphene/Nucleic Acid Interface

The nanobiointerface of graphene and nucleic acids has been characterized by microscopic and many other analytical techniques. Basically, the physical techniques including atomic force microscopy (AFM), transmission electron microscopy (TEM), scanning tunneling microscopy (STM), and X-ray diffraction (XRD), could be applied for the characterization of morphology, structures, crystal structure, chemical compositions and intrinsic properties of the nucleic acid/graphene materials interface.[136] Whereas, optical techniques are most often used to demonstrate the

nanobiointerface of graphene/nucleic acid, including fluorescence spectroscopy and fluorescence resonance-energy transfer (FRET). Besides, electrochemical method is another frequently-used technique which has shown its superiorities in the construction of graphene/nucleic acid interface, which is simple and fast, with low cost and easy operation. And, field-effect transistor (FET) and nanopore are the burgeoning approaches in recent studies, which exhibit great potential in the graphene and nucleic acid-related applications. In this section, we will introduce some cases about the methods/techniques for the characterization and construction of graphene/nucleic acid interface.

4.1 Graphene/Nucleic Acid Interface-based Fluorescence Resonance Energy Transfer

Fluorescence resonance energy transfer (FRET) is a photophysical process based on a non-radiative energy transfer in the fluorescence pair of donor and acceptor. The two components of the FRET pair have an energetic compatibility, where the absorption spectrum of the acceptor overlaps the emission spectrum of the donor. Since the FRET efficiency is dependent on the inverse sixth power of the distance between the donor and acceptor, the two fluorescence molecules have to be in close proximity to allow a significant FRET. Therefore, FRET could promote its versatile application in diverse fields, *e.g.*, to study the conformational dynamic change of biological molecules such as DNA, protein, *etc.*, and to construct variety of biosensing and diagnostic platforms.[137-139] Compared with organic quenchers,

graphene shows superior quenching efficiency for various organic dyes and QDs, with a quenching distance up to 30 nm.[140-144] Theoretical calculations and experimental studies illustrated that both energy-transfer and electron-transfer processes could allow to the deactivation of excited fluorophores on graphene.[142, 143] Along with the selective binding property of graphene to nucleic acids, FRET was often used to investigate the interaction between nucleic acids and graphene surface.[73, 107, 144]

In a typical graphene-based FRET process, graphene is applied in various roles as a substrate in fluorescence quenching detection schemes. The fluorescein-labeled DNA (or RNA) probe was first adsorbed onto the graphene sheet, which results in quenched fluorescence. After adding the target, the fluorescence is recovered due to duplex formation and subsequent desorption. In this process, the fluorophore-to-GO distance increased from zero to infinity to achieve the maximal fluorescence enhancement. Based on these properties, several GO-based sensors have been developed for the detection of DNA, proteins, and other small molecules by using fluorophores-labeled complementary oligonucleotide or aptamer as recognition units.[120, 134, 145-156]

In addition to the fluorescence quenching ability, GO has tunable photoluminescence arising from the small sp^2 graphitic clusters embedded in a sp^3 matrix.[157-165] In the presence of various oxygenous functional groups, GO would open the band gap of graphene. The size of GO can be controlled to within a few nanometers, resulting in tunable photoluminescence properties, and thereby producing a new pathway to develop optical sensors.[157,164-168] For instance, Seo and co-workers demonstrated that the photoluminescence of GO could be quenched by GNPs because

of FRET between GO and GNPs.[166] With the unique photoluminescence properties, the graphene-based photoluminescence sensor promotes its versatile application in the multiplex bio/chemical detection.[164] All together, fluorescence is a highly sensitive technique for the nanobiointerface study on the graphene/nucleic acid.

4.2 Graphene/Nucleic Acid-Based Electrochemistry

Due to its excellent electronic conductivity and electrocatalytic activity, graphene-modified electrodes are showing promising applications in electronics, catalysis, energy storage devices and biosensors. As a single layer of carbon atom in a closely packed honeycomb two-dimensional lattice, graphene can greatly promote the electron transfer rate and electrocatalytic activity owing to its unique properties such as large specific surface area and high mobility of charge carriers. The average electrochemical activity of graphene-modified electrode has been systematically investigated by electron-transfer mediation across modified electrode surfaces.[44, 68, 169, 170].For example, electron-transfer mediation to redox probes, such as $Fe(CN)_6^{3-/4-}$, $Ru(CN)_6^{3-/4-}$, and $Ru(NH_3)_6^{3+/2+}$ have been used to probe the surface electrochemical properties of the graphene-modified electrodes.[170] The results suggested that the existence of graphene could enhance the charge-transfer kinetics and fast the heterogeneous electron transfer,[171-173] possibly owing to the finite density of states of graphene at the redox Fermi energy of the electrochemical probe. Additionally, graphene has exhibited many other advantages such as wide potential windows, relatively inert electrochemistry, excellently electrocatalytic activities with favorable microenvironment. Therefore, the unique 2D crystal structure makes it as extremely

attractive electrode material for the incorporation/interfacing of biomolecules including nucleic acid. Electrochemical techniques such as cyclic voltammetry (CV), differential pulse voltammetry (DPV), electrochemical impedance spectroscopy (EIS), and electrochemiluminescence (ECL) have been used for interfacial investigation of nucleic acid on graphene-based electrode.

4.2.1 Voltammetry.

The electrochemical investigation of DNA bases has been an important field of research, because most of the label-free electrochemical biosensors are based on the redox properties of DNA bases. As its ability for rapid and sensitive detection of single nucleotide polymorphisms (SNPs), direct oxidation of DNA is known as one of the simplest methods for DNA electrochemical analysis,.[174-176] Since Paleček first reported the electrochemical detection of DNA in 1958,[174] a variety of electrodes have been fabricated towards the development of powerful electrochemical DNA sensors. Nanomaterials including GNPs, CNTs and graphene have been demonstrated with improved oxidation signals of the DNA bases in comparison to standard glassy carbon electrodes. As noted, graphene is allowed to interact with DNA molecules through π–π stacking interactions and hydrophobic interactions, thus laying a powerful basis for the application of the graphene/nucleic acid-based interface.[105, 177-182] Zhou *et al.* firstly reported the simultaneous electrocatalysis of all four DNA bases by graphene-based electrode (Figure 1).[177] They employed chemically reduced GO (cr-GO) modified glassy carbon electrodes for electrochemical determining the four bases of DNA (i.e. A, T, C and G), finding that the signals of the four bases were well

separated and enhanced at graphene electrode. Lately, Lim *et al.* found that graphene nanosheets expitaxially grown on SiC could improve the electrochemical response to the DNA bases of dsDNA by anodizing the expitaxial graphene films.[183] Currently, Dubuisson *et al.* showed that based on direct oxidation of nucleotide bases, the anodized epitaxial graphene electrode can detect four DNA bases of ssDNA down to the concentration of nM.[184]

4.2.2 Electrochemical Impedance Spectroscopy.

Electrochemical impedance spectroscopy (EIS) can measure the response of an electrochemical system to an applied oscillating potential as a function of the frequency, which is useful to study the molecular binding process on the nanomaterials-modified electrode. In the EIS studies, the step-wise electrode fabrication process is normally monitored as results of Nyquist plots. The EIS data can be fitted to a Randles equivalent circuit, which includes the solution resistance, electron transfer resistance (*Ret*), the constant phase element and Warburg impedance. In the Nyquist diagram, the diameter of the semicircle reflects the *Ret* of redox conversion of the electroactive marker on the electrode at certain applied potential. This process is strongly dependent upon any modification to the electrode surface.[180] Therefore, EIS has often been used to monitor graphene interfacial property changes upon DNA immobilization and hybridization in label free studies.[185-189]

4.3 Field-Effect Transistor.

Field-effect transistor (FET) devices have attracted much attention in the area of biosensing, due to their sensitivity for molecular interactions. Basically, FET-based

biosensor relies on the biomolecular recognition event at the gate of the FET.[41,190-192] Upon bio-recognition, the electric charge distribution alters the charge carrier density at the surface layer, and thereby changing the channel conductivity. [190-192] Because of its tunable band gap by surface modification, graphene is considered as an ideal material for the construction of FET biosensors. In a typical architecture of graphene-based FET, graphene is deposited on a Si substrate with a 300 nm SiO_2 layer. The doped Si substrate acts as a gate, which induces a surface charge density and thereby shifts the Fermi energy level in graphene. [193] So far, several reports demonstrate that graphene-based FETs with electrolyte top gating can be efficiently used for sensing charged molecules[194-197] Since nucleic acid has a charged phosphate backbone, the graphene-based FET is an ideal tool in the graphene-nucleic acid-based interfacial study and sensing applications.[194-197] For example, Rao *et al.* studied the interaction energies of the nucleobases with graphene using the graphene-based FET. Xu *et al.* recently used CVD-graphene as both electrode and transistor for site-specific detection of target DNA, suggesting a path towards all-electrical multiplexed graphene DNA arrays.[194] Mohanty *et al.* reported the FET-based electrical biosensor using few-layer graphene for the detection of DNA and a bacterium with the covalent-binding DNA probes.[196] Compared with electrochemistry-based signal readout, graphene-based FETs use electrical detection to exploit resistivity change when nucleic acids adsorb on the FET surface, and their microscale, or even nanoscale devices allow to provide better sensing abilities. Thus, these properties make graphene-based FET a promising technique for the interface study.

4.4 Nanopore-Based Analysis.

Nanopore-based analysis is an emerging technique that involves using a voltage to drive molecules through a nanopore in a thin membrane between two electrolytes, and monitoring the ionic current changes through the nanopore as molecules pass through it. Because of the general detection principle and the ease to detect single molecule, the nanopore technology has the significant potential for biosensing applications.[43, 198, 199] With excellent mechanical properties, high electrical conductivity, and surprisingly insulating to ion transport across, graphene-based nanopore appears to be alternative solid nanopore for electronic sensing of DNA molecules, even to distinguish individual base by ion current modulation.[43,200] Up to date, proof of concept to use graphene nanopore for DNA detection has been demonstrated from both experimental and theoretical aspects.[198-204]

Many theoretically works have already addressed such the graphene-based nanopore and verified their feasibility in sequencing DNA[203, 205-208] As calculated, the presence of a nucleobase in the graphene nanopore would affect the charge density, inducing thereby current variations of the order of microampere.[208] And, the controlling the insulating thickness of graphene membrane could dramatically improve the spatial resolution.[204, 209] These calculations indicated that graphene-based nanopore could achieve the single molecule resolution in the DNA analyses.

Experimentally, the improvement of graphene-based nanopore fabrication facilitated the integration of graphene into nanopore technology. In 2008, Drndić and co-workers for the first time fabricated single nanopore and nanopore arrays in

suspended graphene films, and subsequent investigated the kinetics of pore formation and edge stability in graphene.[208] In 2010, Dekker,[206] Drndić,[208] and Golovchenko[209] fabricated the graphene nanopore by using mechanical exfoliation from graphite method or CVD method, separately (Figure 2). In these graphene nanopore, when dsDNA translocated through the graphene nanopore, significant ionic current blockages could be observed. And, the ionic current noise level was several orders of magnitude larger than those in silicon nitride nanopore. As the pore resistance is limited by access resistance at the pore (not by the pore channel itself), it is insufficient to provide sufficient resolution for sequencing when DNA translocating through graphene pore. Merchant *et al.* [208] demonstrated that by means of depositing several nanometers of titanium dioxide over the graphene nanopore, the noise could be significantly reduced. Golovchenko, Dekker and co-workers found that the conductance of the nanopore was related to the pore diameter for graphene membrane, which suggests that the thickness of the membrane was not negligible[204, 210, 211]. Overall, these advancements suggest that graphene-based nanopore could potentially lead to DNA sequencing with electronic readout.[43,197]

There are still various fundamentals about graphene-based nanopore for DNA sequencing or sensing to be explored, however, this preliminary work will certainly facilitate many future studies of graphene nanopore. Their unique properties from graphene would be a big advantage for exploring the graphene-nucleic acid interfacing events.

5. Graphene/Nucleic Acid Interface-Based Bionanotechnological Applications

Nucleic acids are molecules, encoding the genetic instructions, to be used in the development and function of all known living organisms. Due to its base-paired and double helix structure, nucleic acid-mediated assembled/hybridized structures can be designed and controlled as a desirable and reversible manner. Based on the unique electronic and physical-chemical properties of graphene, as well as the interesting adsorption interactions between nucleic acid and graphene, various biosensing platforms with particular characteristics have been developed to facilitate the small molecule detection, immuno-biotechnologies, and DNA sensing/sequencing. We summarize the typical cases and applications of the graphene and nucleic acid biointerface in the following discussions, and list the key elements in the Table 1 and Table 2 for the audience. The developments of the graphene and nucleic acid nanobiointerface is really fast and rapid, audience could look for the original publications or other review articles for more information.[41-44, 53-56, 212]

5.1 Graphene/Nucleic Acid Interface for Biosensing Applications

5.1.1 Heavy Metals

Heavy metals are highly toxic and dangerous pollutants. Some heavy metal pollutants come from fertilizers and sewage, while industrial waste is also the main source of heavy metal pollution. As we know, mercury, lead, and copper are considered as three key pollutes of the most toxic heavy metals. Although there are some available methods for Hg^{2+} detection, ever-growing research efforts have been

devoted to develop unconventional methods for simple and rapid detection of Hg^{2+}.[163, 213] One of the most notable is the Hg^{2+} specific ssDNA sequence which would interact with Hg^{2+} through the formation of a Hg^{2+}-mediated base pair, thymine-Hg^{2+}-thymine. Based on the unique interaction between Hg^{2+} and T rich oligonucleotide, as well as the adsorption between ssDNA and graphene materials, graphene-based biosensors have been utilized for Hg^{2+} detection recently. By using organic fluorephores, sensitive detection of Hg^{2+} was realized *via* fluorescent approaches.[213, 214] A spontaneous fluorescence GO-based sensor with a detection limit of 0.92 nM and selectivity toward Hg^{2+} over other metal ions was designed by Wu and co-workers.[215] By using $[Fe(CN)_6]^{3-/4-}$ and $[Ru(NH_3)_6]^{3+}$ as the electrochemical indicator, Hg^{2+} electrochemical sensors were constructed by Park *et al.* and Zhang *et al.*, respectively.[212, 216] Moreover, GO-based field-effect transistor biosensor has been constructed by Sharon *et al.*[218] The deposition of a tailored nucleic acid with appropriate T mismatches on the GO, yielded active surfaces for the analysis of Hg^{2+}, resulting in sensitive electronic responsing.

Aptamers and DNAzymes are selected as the recognition elements to set up the Pb^{2+} biosensors based on graphene nanomaterials and oligonucleotides. For the cases based on the Pb^{2+} aptamers, fluorescein and quantum dots were used as illuminant whereas GO was employed as the fluorescence quencher. Zhao *et al.* and Wen *et al.* reported graphene-DNAzyme biosensors for Pb^{2+} detections with high sensitivity.[219, 220] Furthermore, Wen *et al.* designed the electrochemical detection method for Pb^{2+} using gold nanoparticle and DNAzyme-functionalized graphene FET.[221] The graphene

decorated with gold nanoparticles serves as the anchoring sites to covalently immobilize thiolated DNAzyme molecules. The Pb^{2+} FET biosensor exhibited a detection limit as 20 pM.

DNAzymes are *in vitro* selected DNA molecules with enzyme-like catalytic activities. Metal ion-dependent DNAzymes are a class of well-characterized DNAzymes that cleave an oligonucleotide substrate containing one ribonucleotide at the cleavage site. Thereby, graphene biosensors with metal ion-dependent DNAzymes have been designed for Cu^{2+} detection with the tremendous progress in graphene nanotechnology. Quan and co-workers designed a label-free fluorescent Cu^{2+} sensor based on internal DNA cleavage and an extrinsic fluorophore in a graphene/DNAzymes complex.[222, 223] Yu *et al.* proposed a GO enhanced fluorescence anisotropy strategy for Cu^{2+} detection with DNAzyme-based assay.[224] A ‘‘turn-on’’ fluorescent method for the direct detection of Cu^{2+} in solutions using molecular beacons and GO was designed by Li and co-workers.[225] In the presence of Cu^{2+}, the molecular beacons were cut into short pieces and released, leading to fluorescence restoration.

5.1.2 Small Molecules

Detection of biological interesting small molecules has fundamental significance in the understanding of cellular functions and pathology, and practical importance in the development of applications in diseases diagnosis and drug discovery. Some biological small molecules including the energy molecules (nucleoside triphosphate), antibiotics, drugs, *etc.* play crucial roles in biochemical reactions or cell functions.

With the developments of graphene based-materials and nucleic acids interface, notable achievements are reported recently to illustrate the sensitive, selective or rapid detection of biochemical interested small molecules.

Small Molecules Detection based on Functional Aptamers. ATP is an important major carrier of chemical energy in living organisms, participating in lots of enzymatic activities.[226] Therefore, detection of ATP has been explored extensively by using graphene-DNA scaffold. Tan and co-workers reported a sensitive and real-time fluorescence anisotropy (FA) detection method for ATP based on graphene signal amplification.[227] Because of the extraordinarily larger volume of GO, ATP labeled with fluorophore exhibits very high polarization when bound to GO (the enhanced FA value was more than 0.5), while the FA was greatly reduced when the aptamer complexes with ATP, which exhibited a maximum signal change of 0.316 with a low detection limit of 100 nM ATP in buffer solution. Another successful example for ATP detection was reported by Liu *et al.* by using upconversion nanophosphors and GO (**Figure 3A**). NIR-to-visible upconversion nanophosphors (UCNPs) are capable of emitting strong visible fluorescence under the excitation of NIR light. Liu *et al.* proposed that GO could quench the fluorescence of ATP aptamer-UCNPs (UCNPs modified with ATP aptamer), and the FRET between UCNPs and GO therefore could be realized. The detection limit of ATP based on the ATP aptamer-UCNPs was as low as 80 nM.[228] Efficient energy acceptance of GO accelerated the researches based on GO assisted fluorescence assays. A molecular aptamer beacon (MAB) containing ATP aptamer and a hairpin-shaped probe were designed by He *et al.* to realize the ATP

detection in A549 cell lysis buffers.[329] In the absence of ATP, the fluorescence of MAB was completely quenched by GO. Upon the adding of ATP, fluorescence was recovered due to the releasing of MAB from GO. The detection limit of ATP in buffer solution was 2 μM.

Electrochemical methods including CV and DPV have been employed for ATP detections.[44] Mesoterakis (4-methoxyl-3-sulfonatophenyl) porphyrin (T (4-Mop) PS4) was used to functionalize graphene sheets *via* π-π interactions to produce T (4-Mop) PS4-graphene hybrid nanosheets (TGHNs).[230] The TGHNs could successfully adsorb ATP aptamer (ATA) on the electrode surface through a π-π stacking. When ATP was added into the system, the electrochemical signal was blocked and the sensitive detection of ATP was realized successfully. The preferable linear range for ATP was from 2.2 nM to 1.3 mM with a detection limit of 0.7 nM.[230] Another interesting case based on the term of graphene-DNA was explored by Wang and co-workers.[231] Taking advantage of strand-displacement DNA polymerization and parallel-motif DNA triplex system as dual amplifications, they designed an electrochemical label-free integrated aptasensor based on silver microspheres as a separation element and graphene-mesoporous silica gold nanoparticle hybrids as an enhanced element of the sensing platform. Through the multiple effects, a low detection limit of 2.3×10^{-11} M was achieved based on the dual signal amplification method.[231]

Diversified sensing platforms for all kinds of small molecules such as cocaine, coralyne, D-vasopressin, mycotoxins, ochratoxin A *etc.,* have been developed with the features of graphene and nucleic acid.[232-239] Detection of cocaine with low detection

limit down to 1 nM was carried out by using two engineered aptamers in connection to redox-recycling signal amplification.[232] The streptavidin-conjugated alkaline phosphatases (ALPs) were used as labels to generate quantitative signals. Du *et al.* utilized GSGHs as magnified sensing platform for D-vasopressin detection, shown as **Figure 3B**.[237] The proposed sensing platform could be used as a chiral selector for distinguishing vasopressin enantiomers at 5 ng mL^{-1} in the presence of L-vasopressin.

Fluorescent techniques on the basis of graphene-DNA structures have been emerging as a new part of the toxin detection field in the recent studies. Utilizing GO as the fluorescence quencher, Wu *et al.* and Sheng *et al.* have developed two FRET aptamer sensors for ochratoxin A (OTA) and fumonisin B1 (FB1), respectively.[238, 239] The OTA FRET sensor based on poly(vinyl pyrrolidone)-coated GO showed the detection limit of 21.8 nM.[239] The FB1 FRET sensor utilizing upconversion fluorescent nanoparticles $BaY_{0.78}F_5{:}Yb_{0.7}Tm_{0.02}$ coated with FB1 aptamers provided a linear range from 0.1 to 500 ng mL^{-1}, and a detection limit of 0.1 ng mL^{-1} for FB1 target.[238] Moreover, the Au-DNA-microcystin complex could be formed through the interaction between ss-DNA modified Au nanoparticles and saxitoxin (STX) or neosaxitoxin (NEO).[239] These microcystins in the complexes could be immunologically recognized by the antibodies adsorbed on GO sheets. As a result, Au NPs were close enough to quench the photoluminescence of GO by FRET. The detection limits were 0.5 and 0.3 μg L^{-1} for STX and NEO, respectively.[240]

Small Molecules Detection based on DNA sequences. A binding mode between DNA and silver ions was utilized for cysteine detection through FRET mechanism

based on GO and dye labeled ss-DNA.[146, 241, 242] These methods basically relied on the competitive ligation of silver ions by cysteine or cytosine-cytosine mismatches in self-hybridizing strand. In the work reported by Liu *et al.*, fluorescence intensity decrease was found to be proportional to the increase of concentration of cysteine in both aqueous buffer (2-200 nM) and human serum (5-200 nM).[243] For the protocol reported by Qu and co-workers, a turn-on assay for cysteine was achieved by using thiol-activatable metallized DNA1, the dye-labeled DNA 2 and GO.[146] The detection limit of cysteine corresponded to 2 nM, and can also be utilized to design the"OR" and "INHIBIT" logic gates using cysteine and DNA as inputs.

Small Molecules Detection based on Nuclease. Nuclease owns special ability for DNA cleavage, and has been founded as a powerful tool for the sensing assays of biotin, theophylline and thiamine pyrophosphate (TPP).[244-248] Exonuclease I is taken as an element for biotin detection. Upon the addition of free biotin, it competes with the labeled biotin for the binding sites of streptavidin and then the exonuclease I digests the unbound DNA probe to release the fluorophore from the DNA, resulting in the fluorescence recovery. The detection limit for biotin was 0.44 nmol L^{-1}. [244] Dnase I was used as an cyclic amplification tool for the detection of ophylline and TPP.[246] In this design, Dnase I could cleave the free DNA in the DNA/RNA ribozyme complex, thereby liberating the labeled fluorophore and ultimately releasing the Shine-Dalgarno sequence from DNA/RNA ribozyme complex. The released Shine-Dalgarno RNA then binds with another probe, and the amplification cycle starts anew, forming a amplided TPP sensing strategy. Another interesting assay method with nuclease was

based on the degradation ability of bleomycins (BLMs) of ssDNA.[247] Similarly, based on the quenching effect of GO, BLM detection could be realized through the degradation of dye labeled DNA with good sensitivity (a detection limit of 0.2 nM) and fast test (within several minutes).[247]

In conclusion, while DNA is kind of functional biological molecule for gene information storage, it is also a useful material for interface constructions of sensors. By taking self-assembly, adsorption, or trapping methods, DNA molecules could be immobilized on the electrode surface with graphene nanomaterials, to set up the sensing electrochemical interface for electrochemical sensing of various small molecules, including dopamine, glucose, histidine, nonylphenol and so on. [236, 242,247-250] The detail building structures and detection performances could be found in the **Table 1**.

5.1.3 Proteins

Proteins perform a vast array of functions within living organisms, including catalyzing metabolic reactions, replicating DNA, responding to stimuli, *etc.*. To date, various sensing methods have been developed for protein assays by using different receptors. Among them, aptamers and immunological recognitions are two significant paths which attract multitudinous attentions in protein biosensing researches. Herein, we have summarized recent works about thrombin and other proteins detection methods based on graphene-DNA complexes.

Proteins Detection based on Electrochemical Methods. Graphene is an ideal electrochemical signal transducer due to its good electroconductibility. For one kind

of thrombin sensors, graphene materials are employed as electrode materials for thrombin aptamer (TA) immobilization. For example, a graphene modified electrode was prepared by chemical reduction of GO adhesived on electrode surface, and TA was linked on graphene/GCE through covalent binding. In the presence of thrombin, a complex of quadruplex-thrombin was formed and such a complex increased the steric hindrance which greatly reduced the signal of $[Fe(CN)_6]^{3-/4-}$.[251] Similarly, the ethanethiol-TA could be attached on Au NPs/graphene electrode surface through S-Au interactions, and thrombin detection could be carried out by using $[Fe(CN)_6]^{3-/4-}$ probe.[252] Additionally, electrochemical impedimetric thrombin sensor has been developed with electrochemical probe.[171] The impedimetric aptasensor showed selectivity for thrombin in the presence of IgG, BSA and avidin. Dong *et al.* reported a method with electroactive dye-Orange II as the electrochemical probe for thrombin detection.[253] This label free electrochemical sensor exhibited a detection limit of 3.5×10^{-13} M and a linear range from 1.0×10^{-12} to 1.0×10^{-10} M.[253] Another label-free electrochemical aptasensor for thrombin employed direct electron transfer of glucose oxidase (GOD) as a redox probe and a gold nanoparticle–polyaniline–graphene (Au–PANI–Gra) hybrid as the substrate to support the GOD probe. TA could be immobilized on gold nanoparticles *via* S-Au bond and realized the sensitive detection of thrombin. [254] As an important growth factor, platelet-derived growth factor (PDGF) aptasensor was developed through sandwich-type aptamer-bindings. Reduced GO sheets were used as matrices to immobilize the GOD and HRP to produce the secondary label. Au NPs functionalized single-walled carbon nanotubes were

employed to modify the working electrode. This method could realize the simultaneous detection of PDGF and thrombin. [187]

By using $Ru(phen)_3^{2+}$ as ECL probe, thrombin ECL sensor was constructed by Wang *et al*.[244] TA was linked on GO modified electrode with amide linkage and hybridized with a complementary DNA containing of $Ru(phen)_3^{2+}$. After interaction with thrombin, the complementary $Ru(phen)_3^{2+}$ probe was released while the detection was achieved.[255] Graphene or GO nanomaterials are considered as favorable nano-carrier for signal amplification and noise reduction in thrombin biosensors. Since thrombin owns dual binding sites corresponding to TA, one thrombin molecule can bind with two TA strands simultaneously. Hence, sandwich-type aptasensor for thrombin detection was built by using graphene derivative as the signal amplification unit in some researches. For an instance, a GOD–functionalized chemically reduced graphene nanosheet was prepared and served as a secondary label through its direct electrochemistry and electro-catalysis in a sandwich-type thrombin electrochemical aptasensor. Bai *et al.* immobilized GOD on GO and prepared a PAMAM–CNTs modified electrode as the working sensing platform (**Scheme shown as Figure 4**).[256] In the presence of thrombin, a sandwich type aptasensor was constructed and the sensitive detection of thrombin was realized based on the dual signal amplification process, with the detection limit of 2.1×10^{-13} M.[256] Similarly, graphene based nanomaterials also served as nanocarriers for different electrochemical labels like alkaline phosphatase and gold nanoparticles mediated silver deposition,[256] hollow CoPt bimetal alloy nanoparticles for HRP adsorption,[257] thionine/hemin/G-quadruplex

bioelectrocatalytic complex and 3,4,9,10-perylene-tetra-carboxylic dianhydride ECL probes.[240, 258,259] All of these cases benefit from the signal amplification effect of the graphene-based secondary label and the sandwich type binding thrombin aptasensor, showing dramatic detection limit and linear responsing range in buffer or sample assays (See **Table 2** for more information).

Proteins detection based on optical methods. Electrochemical methods are major approaches for thrombin detection in the field of graphene–DNA complex. Moreover, colorimetric assay, [260-262] chemiluminescence resonance energy transfer (CRET) system,[263] fluorescence assay, [107] UV-vis spectra,[266] microscopes,[267] and surface plasmon resonance (SPR) have been utilized for thrombin aptasensor studies. Guo and co-workers reported a detection method based on DNA functionalized GNPs which could combine with thrombins. The thrombin molecules acted as linkers for GNPs, showing the distance-dependent optical properties.[264] Bi *et al.* developed a GO platform based on the luminol–H_2O_2–HRP-fluorescein CRET system (**Figure 5A**).[263] Luminol acts as both chemiluminescence substrate and donor, and fluorescein as both enhancer and acceptor. Li's group designed a FRET aptasensor for thrombin detection based on the unique assembly interaction between ss-DNA and sodium dodecyl-benzene sulfonate functionalized graphene. The graphene FRET aptasensor is extraordinarily sensitive to the thrombin detection with high specificity in both buffer and blood serum (**Figure 5B**).[107] Furukawa *et al.* demonstrated that the elementary processes of protein recognition could be observed directly with a confocal laser scanning microscope and an AFM using an identical piece of GO.[265] They also

showed that the recognition system could be installed and operated in microchannel devices.[265] For another example, well dispersed graphene, prepared by the chemical reduction of GO with hydrazine, was assembled on a positively charged SPR Au (p-Au) film *via* electrostatic interaction. TA could adsorb onto the graphene layer through the strong noncovalent binding of graphene with nucleobases. Binding between the aptamer and the target molecule greatly disturbed the interaction between the aptamer and graphene. As a result, TA was released from the SPR sensing surface and an obvious SPR angle decrease could be observed.[266] Lysozyme detection was carried out with electrochemical, fluorescence and SPR monitoring.[92, 266-268] The SPR sensor consists of a 50 nm gold film coated with a thin film of reduced graphene oxide (rGO)-functionalized with anti-lysozyme DNA aptamer, with a detection limit of 0.5 nM.[92]

Proteins detection based on FET method. By using large-area CVD derived graphene, a micron-scale graphene FET biosensor has been produced. The chips were treated with pyrenebutanoic acid succinimidyl ester and TA. This graphene-aptamer FET sensor can be used to monitor protein–aptamer binding in real time.[269] By growing polypyrrole-converted nitrogen-doped few-layer graphene (PPy-NDFLG) on Cu substrate by CVD, a VEGF (Vascular endothelial growth factor, VEGF) FET sensor was fabricated with VEGF RNA aptamer on liquid-ion gated FET geometry by Kwon *et al.* (**Figure 6**). [270] A 100 fM detection limit was obtained for VEGF by this method. Immunoglobulin E (IgE) FET sensor was reported early by Ohno *et al.* [271] The label-free immunosensor based on an aptamer-modified graphene FET showed

selective electrical detection of IgE protein. From the dependence of the drain current variation on the IgE concentration, the dissociation constant was estimated to be 47 nM, indicating good affinity and the potential for graphene-based FETs to be used in biological sensors.

Overall, based on the synergistic effect of DNA and graphene, as well as the multiple functions of aptamers and DNAzymes, various protein sensors have been constructed in the past few years to realize the sensitive and selective protein assays. Among them, thrombin is the most popular target for major researches, due to its clear structure, significant role, and unique dual binding sites for aptamer. Moreover, other proteins such as IgE, lysozyme, VEGF, PDGF, interferon-gamma, folate receptor, α-chymotrypsin, epithelial tumor marker mucin 1, and nuclear factor-kappa B (NF-kB) have been taken as the analytes to test the graphene-DNA sensing interface in the form of biosensors. We summarize the examples shown in the existed publications and listed the detail information in Table 2.

5.1.4 Nucleic Acids

In the nucleic acids electrochemical sensing, the electocatalytic performances are strongly relied on the surface chemistry of biosensors, as well as the signal transduction abilities. As the researches of graphene based materials going further, more and more papers can be found in connection with nucleic acids detection, based on its unique electronic properties including high integer quantum Hall effect, the Klein paradox, an ambipolar electric field effect, along with ballistic conduction of charge carriers, *etc.*. Herein, we will focus on the studies about graphene derived

materials for DNA detection with electrochemical, fluorescence, and chemiluminescence methods, as well as various techniques including colorimetric analysis, transistors, Raman scattering, mass spectrometry, *etc.*.

Nucleic acid detection based on Electrochemical Detection. Among various methods for electrochemical nucleic acid biosensors, the label free ones own the simple, fast and easy operations characteristics. Akhavan *et al.* prepared a GO nanowalls with extremely sharp edges and deposited them on a graphite electrode by using electrophoretic deposition in an Mg^{2+}-GO electrolyte.[103] Detection of oligonucleotides with specific sequences (the sequence from codon 248 of the p53 gene) was realized with the detection limit of 9.4 zM (5 dsDNA per mL). A microwave-assisted sulfonation was employed to prepare water-soluble sulfonated reduced graphene oxide (srGO) to set up a srGO-DNA biosensor.[272] The solution of srGO-DNA hybrids was dropped onto the surface of an interdigitated gold electrode for the assembly of electrochemical DNA sensing platforms.

As a classical electrochemical probe, $[Fe(CN)_6]^{3-/4-}$ has been widely used in the electrochemical biosensors to indicate signal changes. For example, $[Fe(CN)_6]^{3-/4-}$ can detect the target gene strands hybridized with probe DNA on the electrode surface because of the electroconductivity. Based on the rGO and poly(m-aminobenzenesulfonic acid, ABSA) nanocomposite (PABSA-rGO), Yang *et al.* reported a sensitive detection method for PML/RARA fusion gene sequence.[161] The dynamic detection range for the sequence-specific DNA was from 1.0×10^{-16} to 1.0×10^{-8} mol L^{-1}. Jayakumar *et al.* synthesized a first generation (G1)

poly(amidoamine) dendrimer (PAMAM) with graphene core (G@G1PAMAM), and then immobilized G@G1PAMAM covalently on mercaptopropionic acid (MPA) monolayer on Au electrode.[273] Au nanoparticles (17.5 nm) were decorated the G@G1PAMAM and used for electrochemical DNA hybridization sensing with the help of $[Fe(CN)_6]^{3-/4-}$. Another important apllication of $[Fe(CN)_6]^{3-/4-}$ probe is for EIS assays. The probe could be reduced and oxidized on the electrode surface then transduce the surface changes into electrochemical signals. In the existed publications for DNA electrochemical sensors by using graphene based materials, 1-aminopyrene,[274] GNPs linked p-aminothiophenol functionalized GO,[275] N,N-bis-(1-amino propyl-3- propylimidazol salt)-3,4,9,10-perylene tetracarboxylic acid diimide (PDI),[197] and poly(xanthurenic acid) were used to prepare the functional graphene hybrids for fabricating label-free electrochemical impedance genosensor.[276] Based on the modifications, probe nucleic acids could be anchored on the functionalized graphene surface, and with the hybridyzations of target nucleic acids, and $[Fe(CN)_6]^{3-/4-}$ probe can report the impedance changes. Methylene blue is a phenothiazine dye and commonly used electrochemical indicator in the electrochemical DNA biosensor, to monitor the DNA hybridization reaction.[277-279] An anodized epitaxial graphene electrode was used for the detection of 30 mer oligonucleotides as a demonstration to illustrate the higher sensitivity of graphene based sensor than anodized graphite in terms of electrochemical sensing, and the results based on EIS technique are shown as **Figure 7**.[194] Transgenic soybean A2704-12 gene sequence could be detected on a partially reduced GO modified

carbon ionic liquid electrode (CILE).[280] The CILE was fabricated by using 1-butylpyridinium hexafluorophosphate as the binder and probe DNA was connected *via* covalent bond. Another transgenic soybean sequence of MON89788 was detected on graphene and TiO_2 nanorods composite film.[281] Under optimal conditions the differential pulse voltammetric response of the target ssDNA sequence could be detected in the range from 1.0×10^{-12} to 1.0×10^{-6} mol L^{-1} with a detection limit of 7.21×10^{-13} mol L^{-1}. Furthermore, adriamycin was used as intercalated indicator when the probe DNA (anchored on graphene modified electrode) hybridized with the target DNA. The peak currents of adriamycin or daunomycin were linear with the concentration of complementary DNA, resulting in sensitive detection of gene sequence.[282]

The ssDNA is a common probe for the target DNA detection with the complementary sequence on the principle of bases matches. Moreover, molecular beacons and peptide nucleic acid (PNA) are also promising probes for the target DNA sensing with their high specifities. PNA, whose sugar-phosphate backbone is replaced with a peptide-like backbone, is neutral, which eliminates electrostatic repulsion between the two hybridized strands.[293] Hairpin-DNA is a secondary DNA structure in which two regions of the same strand, complementary in nucleotide sequence, base-pair between each other to form a double helix that ends in an unpaired loop. Pumera and co-workers designed an EIS sensor with the hairpin-shaped DNA probes for detection of single nucleotide polymorphism correlated to the development of Alzheimer's disease.[283] Chen *et al.* developed an enzyme-assisted target recycling for

amplified EIS detection of DNA on a graphene/GNPs modified electrode with hairpin-shaped DNA probe.[275] PNA probe has been demonstrated with effective recognition ability for target DNA sensing by and co-workers through a GO modified electrode transducer. [293] The strategies for signal amplification by using HRP enzymatically electrochemisty,[284] and strand-displacement DNA polymerization have shown their dramatic effects on improving the sensitivity of sandwich-type DNA biosensors with graphene derivative modified electrodes.[285] Under the synergistic effect of the biobarcode signal amplification and catalytic current enhancement as well as the fast electron transfer on the graphene modified electrode, low detection limit of target DNA sequence was successfully achieved.

Nucleic acids detection based on FRET method. Compared with traditional organic quenchers, graphene derivatives have shown superior quenching efficiency for a variety of fluorophores, with low background and high signal-to-noise ratio, as well as the unique protection from enzymatic cleavage. In the recent studies, GO and GO-based complexes with 4-(1-pyrenyl-vinyl)-N-butylpyridinium bromide (PNPB), $[Ru(bpy)_2(pip)]^{2+}$ (bpy=2,2'-bipyridine; pip=2-phenylimidazo [4,5-f] [1,10] phenanthroline), rhodamine 6G, ethidium bromide (EtBr), and poly [(9,9-bis(6'-N,N,N-trimethy lammonium) hexyl)-fluorenylene phenylene dibromide] (PFP) have been employed as FRET sensing platform for DNA sensitive detection.

By using $Ru(bpy)_2(pip)]^{2+}$, the Ru^+ compound can interact with dsDNA or G-quadruplex DNA structure and result in the fluorescene recovery. The concentration of 0.25 μM dsDNA can be detected with the

$Ru(bpy)_2(pip)]^{2+}$/G-quadruplex biosensor.[286] In another case, EtBr, a common fluorescence tag (or nucleic acid stain) was employed.[287] EtBr owns the conjugated "π" structure which can adsorb on graphene surface, resulting in the fluorescence quenching. When EtBr interacted with dsDNA, the fluorescence could be "turn on" fleetly. The competition between DNA/dye and graphene/dye was considered as a effective tool for constucting the DNA biosensors. A cationic conjugated polymer PFP and rhodamine 6G was used to modify the graphene nanomaterials to produce the functionalized graphene derivative.[288,289] In the presence of target DNA samples, the interaction between functionalized graphene derivative and dye was disturbed. For the case by using PFP, a detection limit of 40 pM for target DNA detection was realized with a traditional PFP-based DNA sensor by introducing GO as a quencher.[288] For rhodamine 6G (R6G) case, the addition of DNA can restore the fluorescence signal of R6GGO complex by binding with R6G and removing it from the surface of the GO. The detection limit for DNA was 0.01 nM and the precision for eleven replicate detection was 3.8%.[289] MBs and PNA have shown the remarkable applications in graphene based DNA biosensors. The researchers make use of these FNAs as the probes to hybridize with target DNA.[290] Moreover, GO owns large surface/volume ratio, as well as the 2D planar structure. These unique properties make GO as a ideal multiple sensing platform for colorful detection systems with more than one target. Tao *et al.*, Qu *et al.*, Zhu *et al.*, and other scientists have built up the multicolor fluorescent DNA biosensors with the help of graphene based nanomaterials.[142, 147,291,292]

The fundamental investigations of nucleic acids-graphene sensing systems provide rich information and well element task for further applications of DNA/graphene biosensors in logic gate operations and array imaging. To the advanced DNA/graphene biosensors, different biological agents like exonuclease III (ExoIII) and biochemical approaches like toehold-mediated strand displacement and isothermal circular strand-displacement have been introduced into the systems. Tan and co-workers developed a DNA assay based on ExoIII-induced target recycling and the fluorescence quenching ability of GO.[294] Introduction of target sequence induces the ExoIII catalyzed probe digestion and generation of single nucleotides. After each cycle of digestion, the target is recycled to realize the amplification. Ihara and co-workers immobilized dye-labeled probe DNA on GO through a capture DNA probe.[295] When targets were added, the probes were released from the GO through toehold-mediated strand exchange. High emission recovery and good signal contrast were achieved relative to conventional methods that were based on direct adsorption of probes. A label-free fluorescent DNA biosensor with isothermal circular strand-displacement polymerization reaction combined with GO binding was presented by Yu's group.[296] The proposed method is simple and cost-effective with a low detection limit of 4 pM. Cerf and co-workers reported the transfer-printing of ss-DNA molecule arrays on graphene for the high resolution electron imaging by using capillary assembly procedure.[297] This method might be an efficient step toward the observation of single elongated DNA molecules with single base spatial resolution to directly read genetic and epigenetic information.

Nucleic acid detection based on chemiluminescent method. Chemiluminescence is a powerful detection technique in addition to fluorescence. DNA biosensors have been designed based on CRET in the system of luminol-H_2O_2-HRP-fluorescein and luminol-H_2O_2-DNAzymes.[297-300] The CRET biosensor for human immunodeficiency virus (HIV) oligonucleotide sequence detection showed a detection limit of 34 pM,[301] whereas the ExoIII-assisted target recycling amplification CRET biosensor for DNA detection achieved a detection limit of 9 fM in 2.5 h.[299] They demonstrated that guanine, with a 10-fold higher transverse conductance, could be singled out from the other bases.

Nucleic acid detection based on other techniques. Girdhar *et al.* and Hyun *et al.* reported the DNA sensing and conformation monitoring by using graphene based solid-state nanopore.[301,302] Graphene can also be used as an substrate for Surface Enhanced Laser Desorption Ionization-Time of Flight-Mass Spectrometry (SELDI-TOF-MS) and for SERS.[297,303] A SERS-active substrate based on Au NPs-decorated CVD-growth graphene was used for multiplexing detection of DNA. Due to the combination of GNPs and graphene, the Raman signals of dye were dramatically enhanced.[297] This platform exhibited extraordinarily high sensitivity and excellent specificity for DNA detection, showing a detection limit as low as 10 pM.

5.1.5 Single-Nucleotide Polymorphism, DNA Cleavage, DNA Damage and Repair

Analysis of single-nucleotide polymorphism (SNP), DNA cleavage, DNA damage and repair is in high demand not only because of the important part they play in preventing diseases, selecting medicines, developing new medicines and vaccinating

diseases, but also in studying the genome structure and function. In the following part, we will talk about the recent achievements about graphene based DNA biosensors in the applications of SNP, DNA cleavage, DNA damage and repair.

Single-base specific hybridization. Classical methods for sequence-specific recognition of DNA are based upon the DNA hybridization between two complementary ssDNA, which require denaturing dsDNA prior to the research. By introducing graphene nanomaterials into this topic, single-base specific hybridization can be monitored through fluorescent, electrochemical and electronic methods. Electrochemically reduced graphene oxide (ErGO) and GNPs were prepared to fabricate the GNPs/ErGO composite film covered glassy carbon electrode for the electrochemical method. The resulting GNPs/ErGO/GCE was demonstrated with good sensitivity for A, T, C, and G bases.[304] By transferring the CVD-grown graphene films from Ni to glass substrates, a large-sized graphene transistor was fabricated and used for hybridization of target DNAs to the probe DNAs pre-immobilized on graphene with detection sensitivity of 0.01 nM and capability to distinguish single-base mismatch.[305] These studies demonstrate the emerging potentials of graphene based biosensors in sensitive and readily detection of SNPs or mutation that is thought as the key to diagnosis of genetic diseases and realization of personalized medicine.

Single nucleotide polymorphism detection. Human genome mutations are the key factors in genetic disorders, predisposition to diseases, and discrepancies in the response to drugs and therapeutics. With the development of genetic therapy, clinical

diagnosis and molecular biology, SNP is regarded as not only a genetic marker in the study of cancer-related drug metabolism or reactivity, but also a fundamental tool in the identification of inherited disease-causing genes. Pumera *et al.* used GO nanoplatelets as electroactive labels for DNA SNP detection.[306] The working signal comes from the reduction of the oxygen-containing groups on the surface of GO. Dong and co-workers developed a wet-chemical strategy for synthesizing hemin-graphene hybrid nanosheets (H-GNs) and reported the H-GNs based label-free colorimetric detection system for SNPs.[261] Graphene-based platform for SNP genotyping was also realized with fluorescent technique. Under the assistance of DNA ligase for linkage catalyzing or polymerase for dGTP-single base extension, the FRET SNPs biosensor was fabricated.[147, 307] A microfluidic chip for SNP genotyping using GO and a DNA intercalating dye was designed by Li *et al.*[308] Under optimized conditions, they could detect 1 nM DNA with 0~10 nM linear range and differentiate 5% SNP. Through a microarray-based solid phase assay, a 0.25 pmol DNA detection limit and 0.5 pmol single-base mismatch sequence discrimination could be achieved in a visible manner. [308]

DNA damage detection. DNA lesions are a primary cause which will induce the final mutation of DNA sequence, resulting in the gene information confusion. In the past decades, along with the developments of graphene-based biosensors in DNA detection and analysis, several typical experiments have been implemented for DNA damage and repair screening. Sidorov *et al.* reported the use of a sensitive CVD graphene platform for controlled and enhanced sequence-dependent low-energy

electron-induced DNA damage studies.[309] With the SERS provided by graphene adsorbed on Au thin films, this sensing strategy allows direct, rapid assessment of ≤1 eV electron-induced DNA damage as a function of base sequence. Zhou *et al.* reported a homogeneous assay platform for DNA base excision repair screening with graphene oxide-hairpin probe nanocomposite[310] A dynamic range from 0.0017 U mL^{-1} to 0.8 U mL^{-1} was achieved for uracil-DNA glycosylase assay.[310]

DNA methylation detection. DNA methylation is an important epigenetic event which refers to methyltrans-ferase (MTase)-catalyzed covalent addition of a methyl group to adenine or cytosine residues in the specific DNA sequence.[311] Li *et al.* presented an electrochemical method for gene-specific methylation detection and MTase activity assay using HpaII endonuclease.[181] The assay was from the electrochemical responses of the reporter (thionine), which was conjugated to 3'-terminus of the probe DNA *via* GO, after the DNA hybrid was methylated (under catalysis of M.SssI MTase) and cleaved by HpaII endonuclease (a site-specific endonuclease recognizing the duplex symmetrical sequence of 5'-CCGG-3' and catalyzing cleavage between the cytosines). This model can determine DNA methylation at the site of CpG and has an ability to discriminate the target DNA sequence from even single-base mismatched sequence.

MicroRNAs detection. MicroRNA (miRNA) is a group of small endogenous noncoding RNAs (approximately 18-25 nucleotides), which encodes in the genomes of different species. Several hundred miRNAs are encoded in the human genome and dozens have now shown to regulate a diverse variety of cellular processes, both in

normal physiology and in disease. Hence, reliable monitoring of miRNAs has great significance, not only for diagnostic and prognostic markers but also for therapeutic intervention. Graphene based fluorescent and electrochemical biosensors have been illustrated. Cui *et al.* realized the multiplex microRNA analysis in complex biological samples based on a cyclic enzymatic amplification method.[121] Dong *et al.* made use of isothermal strand-displacement polymerase reaction to carry out selective multiple miRNA detection based on fluorescence quenching of GO.[149] With site-specific cleavage of an endonuclease, Tu *et al.* reported a miRNA assay which could detect 3.0 fM miR-126 with a linear range of 4 orders of magnitude.[312] Hybridization chain reaction coupled with a GO surface-anchored fluorescence signal readout pathway has been utilized for miRNA detection.[313] An electrochemical biosensor with graphene, sulfydryl functionalized locked nucleic acid (LNA) and molecule beacon was constructed by Yin *et al*.[314] LNA probe and molecular beacon probe were used as the capture probes fro miRNA, whereas the biotin functionalized signal DNA and Au NPs were used as the signal source for miRNA detection. This biosensor showed a detection limit of 0.06 pM.

5.1.6 Bacteria and Pathogens

A potentiometric aptasensor based on chemically modified graphene and aptamers was prepared by Hernandez *et al.* for the detection of living *Staphylococcus aureus*.[315]A single colony-forming unit (CFU)/mL of *Staphylococcus aureus* in an assay close to real time could be realized, offering ultra-low detection limits in very short time responses in the detection of microorganisms. Another aptamer with high

affinity against *Salmonella typhimurium* was reported by Duan *et al.*[316] The authors selected from an enriched oligonucleotide pool by a whole-cell SELEX process in a method for the fluorimetric determination using a GO platform. The fluorophore could be released from the GO due to the formation of the target/aptamer complexes, fluorescence intensity is substantially increased. A detection limit of 100 CFU/mL was achieved and displayed large potential with respect to the rapid detection of bacteria.[316] Food and water borne pathogens have been identified as major cause of infectious disease in humans worldwide. Typhoid, a life threatening illness, is caused by an important food-borne intracellular pathogen *Salmonella enteric serovar Typhi* (*s. Typhi*). Singh *et al.* prepared a GO-chitosan nanocomposite (GO-CHI) electrochemical DNA biosensor and realized the sensitive detection of typhoid.[317] The typhoid biosensor was fabricated by covalent immobilization of *s. Typhi* specific amine labeled ssDNA probe on GO-CHI/ Indium Tin Oxide (ITO) *via* glutaraldehyde. The ssDNA/GO-CHI/ITO biosensor showed a detection range of 100 fM to the typhoid gene in serum samples, indicating the promising applications of graphene based DNA biosensors in biomedicines and clinics. Zuo *et al.* developed a polydimethylsiloxane (PDMS)/paper/glass hybrid microfluidic system integrated with aptamer-functionalized GO biosensors for simple, one-step, multiplexed pathogen detection.[318] The paper substrate used in this hybrid microfluidic system facilitated the integration of aptamer biosensors on the microfluidic biochip, and avoided complicated surface treatment and aptamer probe immobilization in a PDMS or glass-only microfluidic system. *Lactobacillus acidophilus* was used as a bacterium

model to develop the microfluidic platform with a detection limit of 11.0 CFU/mL. Additionally, simultaneous detection of two infectious pathogens-*Staphylococcus aureus* and *Salmonella enterica* was realized on the prepared system. This pathogen assay protocol was in a ready-to-use microfluidic device and could finish the test in 10 min (**Figure 8**). In conclusion, great efforts have been devoted to the detection of metal ions, bacterial, pathogen gene, *etc.* due to their possible threat to public health or ecosystems.

5.2 Graphene/Nucleic Acid Interface for Biomedical and Bioimaging Applications

5.2.1 Detection of Live Cells.

Early detection of carcinoma cells is important for clinical cancer diagnostics. However, highly sensitive and selective detection of cancer cells is still a challenge for the diagnosis and treatment. Recently, graphene/aptamer based biosensors have attracted lots of interests in the scientific research. For the electrochemical biosensors reviewed in the present article, graphene materials were modified on the electrode surface with 3,4,9,10-perylene tetra-carboxylic acid (PTCA) and tris(1-chloroethyl) phosphate (TCEP). After the fabrication of sensitive electrochemical interface, aptamers for the tumor maker mucin 1 proteins (MUC-1 aptamer) and nucleolin (AS1411 aptamer) were linked onto the graphene modified electrode through covalent binding.[319] The aptasensor for MCF-7 cells by using porous GO/Au composites and porous PtFe alloy shows a detection limit of 38 cells/mL, while the AS1411 aptasensor designed by Qu *et al.* showed its promising detection ability for various

cell lines including HeLa cells (human cervical carcinoma cell), MDA-MB-231 (human breast cancer cell), K562 cells (leukemia line), and NIH3T3 cells.[321]

ECL methods combined with QDs or bis(2,2'-bipyridine)-(5-amino-phenanthroline) ruthenium bis(hexafluorophosphate) (Ru1) were utilized as the detection approach for living cancer cells. Jie *et al.* invented an endonuclease-assisted amplification technique using Fe_3O_4/CdSe composite QDs as signal probe.[322] The detection limit was 256 cells/mL with RSD of 5.7%. Wei *et al.* proposed an ECL-FRET method for living cell detection.[323] A multiplex microfluidic chip integrated with the GO-based FRET strategy was designed by Cao *et al.* to create a screening assay for tumor cells. [343] The *in situ* detection of CCRF-CEM cells (T-cell acute lymphoblastic leukemia cells) by assaying the cell-induced fluorescence recovery from the GO/FAM-Sgc8 was recorded on the biosensor with the detection limit about 25 cells mL^{-1}.

5.2.2 Living Cell Imaging

Living cell imaging based on graphene-nucleic acid complex has shown its growing fashion in the live cell studies.[150,323,325] An aptamer–FAM/GO nanosheet (aptamer-FAM/GO-nS) complex has been designed for *in situ* molecular probing of ATP in JB6Cl41-5a mouse epithelial cells.[73] The aptamer-FAM/GO-nS complex, coupled with a wide-field fluorescence microscope, serves as a real-time sensing platform. ATP recognition by the ATP aptamer has been used as a model system to elucidate certain properties and advantages of the GO nanosheet. Moreover, Wang *et al.* further developed a multiple nucleotides detection method based on

DNA/RNA-GO-nS nanocomplex.[134] This is the first demonstration of *in situ* simultainous monitoring of ATP and GTP in living cells (schematically illustrated in **Figure 9A**). The capability of graphene for DNA protection from cleavage during cellular delivery has demonstrated that graphene based-materials can be used as oligonucleotide probes in conjunction with GO-nS to deliver DNA to HeLa cells.[132] Ryoo *et al.* developed a nanosized graphene oxide (NGO) based miRNA sensor, which allows quantitative monitoring of target miRNA expression levels in living cells.[326] The strategy was based on noncovelent binding between NGO and PNA probes, resulting in fluorescence quenching of the dye that was conjugated to the PNA, and subsequent recovery of the fluorescence upon addition of target miRNA. The miRNA sensor allowed the detection of specific target miRNAs with the detection limit as 1 pM. A one-step, protein-directed approach for preparing the functional rGO with herceptin was proposed by Irudayaraj and co-workers.[327] As both a reducing and stabilizing agent, herceptin was attached onto the GO sheets where it also reduced the GO. The rGO-herceptin exhibited near-infrared excitation characteristics and non-photobleaching properties which are promising for live cell imaging. Incubation of the novel rGO-herceptin composite with SK-BR-3 cells was then monitored by imaging technique. Chu and co-workers reported an strategy for caspase-3 activation imaging in live cells with GO-peptide conjugate as an intracellular protease sensor.[328] Confocal fluorescence microscopy experiments with HeLa cells suggested that the GO-peptide conjugate was efficiently delivered into live cells and acted as a “signal-on” intracellular sensor for specific, high-contrast imaging

of caspase-3 activation. Akhavan *et al.* applied rGO nanoribbons functionalized by amphiphilic polyethylene glycol (rGONR-PEG) to attach arginine-glycine-aspartic acid (RGD)-based peptide and cyanine dye 3 (cy3) for targeting $\alpha_v\beta_3$ integrin receptors on human glioblastoma cell line U87MG.[67] Confocal fluorescence imaging of cancer cells with the rGONR–PEG–cy3–RAD was final realized with confocal microscope.

5.2.3 Gene Delivery, Gene Silence and Therapy.

Up to date, various novel nanomaterials have been merging as functional vectors for gene delivery in living cells to realize the gene silence and gene therapy. Due to the dramatic physical, chemical, electical and optical features, graphene and the derivatives (including GO, chemically reduced graphene, functional graphene based nanomaterials) have been employed as the advanced vectors for gene delivery. Some successful explorations have been reported so far and we would like to summarize some typical cases in the following content. Feng *et al.* prepared polyethylene glycol (PEG) and polyethylenimine (PEI) conjugated GO *via* covalent amide bonds.[329] The resulted dual-polymer-functionalized nano-GO conjugate (NGO-PEG-PEI) obtained a physiologically stable with ultra-small size. The authors used NGO-PEG-PEI to deliver small interfering RNA (siRNA) into cells under the control of NIR light, resulting in obvious down-regulation of the target gene, Polo-like kinase 1 (Plk1), in the presence of laser irradiation. Chen *et al.* fabricated the gene delivery system based on GO chemically-functionalized with branched polyethylenimine (PEI-GO).[330] They evaluated the transfection efficiency of PEI-GO and demonstrated that the luciferase

expression of PEI-GO was comparable or even higher than that of the PEI 25 kDa at optimal mass ratio. Moreover, they found PEI-GO could effectively deliver plasmid DNA into cells and be localized in the nucleus. PEI functionalized graphene nanomaterials have also been used for delivering the GFP specific siRNA (resulted in 70% suppression of the target gene expression),[331] the molecular beacon for recognition of miRNA,[332] the NLS (nuclear localized signals) peptide PKKKRKV (PV7, one of the primary NLS peptides),[333] multifunctional DNAzyme in living cells,[334] and the enhanced green fluorescent protein plasmid (pEGFP) reporter gene in zebrafish embryos.[335] For example, Kim *et al.* developed a multifunctional DNAzyme delivery system based on nGO for simultaneous detection and knockdown of the target gene (shown as **Figure 9B**). The DNAzyme/GO complex system allowed convenient monitoring of hepatitis C virus (HCV) mRNA in living cells and silencing of the HCV gene expression by Dz-mediated catalytic cleavage concurrently.[334] The gene delivery study is an interesting topic, which has attracted lots of attentions recently. Audience could go to **Table 3** to find more detail data. These findings suggest that functionalized graphene could be a promising nano-vector for efficient gene delivery with high transfection efficiency, hopeful for future applications in non-viral based gene therapy.

5.2.4 Drug Delivery.

Zhang *et al.* realized the sequential delivery of siRNA and anticancer drugs (doxorubicin, DOX) using PEI-grafted GO.[69] The effective delivery of siRNA and

anti-cancer drugs by PEI-GO exhibited a synergistic effect, which led to a significantly enhanced chemotherapy efficacy. Liu, *et al.* synthesized phospholipid monolayer membrane functionalized graphene and tested its applications for drug delivery. [336] Recently, Mohapatra and co-workers reported a chitosan functionalized magnetic graphene (CMG) nanoparticles platform for simultaneous gene/drug and SPIO (superparamagnetic iron oxide) delivery to tumor.[337] CMGs efficiently deliver plasmid DNA into A549 lung cancer cells and C42b prostate cancer cells. These results indicated that CMGs provided a robust and theranostic platform for tumor-targeted co-delivery of drugs, genes and Magnetic Resonance Imaging (MRI) contrast agents. Successful functionalizations of graphene with various inspired materials to be a robust vectors for drug delivery in different cell lines. These research achievements will encourage the development of targeted cancer chemotherapy.[338]

6. Conclusion and Perspective

The combination of nanostructures with biomolecules yields functional nanostructured biointerfaces with synergistic properties and functions. One recent surge of research interest in the nanobiotechnological field is focused on the advanced design and preparation of graphene-nucleic acids nanostructured biointerfaces, as well as the fundamental understanding of the interfacial properties and applications. Since its discovery in 2004, graphene has been considered as one of the most important building blocks for the exploration and fabrication of the nano/bio interfaces, because of their unique structural, physical, chemical, electronic, and mechanical properties.

In the past few years, the integration of biomolecules with graphene has been substantially advanced. Here we summarize the recent advances on the fabrication and exploration of graphene-nucleic acids nanobiointerface, as well as their nanobiotechlogical applications in biotechnology, including various biosensing and biomedical applications, drug delivery, cell imaging, gene delivery and therapy.–

However, there are still many challenges about graphene/nucleic acid nanobiointerface. One of the major challenges primarily stems from the batch-to-batch heterogeneity in graphene preparation. Preparation of functional graphene with tailored surfaces, morphology control and nanostructure definition is considered as key points for graphene manufacturing. For example, the surface oxygen-containing groups on GO lead to good stability and well biocompatibility with biomolecules, while the unquantified amount of defects would reduce the crystal quality and electrical conductivity. Apparently, developing a reliable and scalable fabrication technique and methodology for mass-producing identical graphene and integrating biomolecules to graphene with high yields are some of the technical issues to be addressed in future.

As the expanding of the applications of graphene-nucleic acids nanobiointerface in chemical/biomedical sensing and imaging, the general population is more likely to be exposed to graphene either directly or indirectly, which has prompted considerable attention about human health and safety issues related to graphene. So, before graphene-based bioconjugates can be safely used for *in vivo* biological sensor applications, especially when human bodies are involved, a large amount of work is

needed to be done to clarify the long-term exposure effects and their methods of creation to different cells, tissues, and organs. Although considerable experimental data related to graphene toxicity at the molecular, cellular, and whole animal levels have been published, the results were often conflicting. Therefore, to establish standardized and reliable methods for evaluating the biological effects including toxicity of graphene-nucleic acids biointerface is needed but has not yet been developed, which would be of profound significance to *in vivo* and *in vitro* applications of graphene. Furthermore, so far, most of the measurements were carried out in ideal environment, such as pure buffer solutions. Clearly, the real physiological sample is far more complex and will absolutely draw into a range of interfering and fouling effects, which remains challenging in biomedical applications.

Additionally, better understanding of the interactions methodology of nucleic acids at the graphene interface and of the resulted biological effects will play an important role in applying graphene as a nanoscaffold in biosensing, bioimaging, and drug delivery. It is illustrated that studying the adsorption and orientation of DNA on graphene will provide further understanding of interactions mechanism of graphene with molecules and bio-interfacial properties, which could, in turn, facilitate advances in graphene science and biotechnological applications. For example, the relative ease of integrating graphene into solid-state nanopore platforms toward DNA analysis adds prospects of their use as a sensing technology outside research laboratory in the future.

Despite a number of remaining challenges, the latest progresses on the field of

graphene biointerfacing with nucleic acids have been significant achieved toward the investigation and applications in a wide range of areas. Because the field is still at its early stage, it is expected to branch out the study of graphene biointerfacing with nucleic acids into many applications to meet the needs of society in the areas of safety, enhanced health care, as well as sustainable environment.

Acknowledgements

The authors are grateful for support from the National Natural Science Foundation of China (No. 21235004, No. 21327806, No. 21305046, No. 61405176) and National Basic Research Program of China (No. 2011CB935704), Natural Sciences Funds of Zhejiang Province (LY14B05004), and Tsinghua University Initiative Scientific Research Program and Fundamental Research Funds for Central Universities.

Table 1. Small molecules detection based on graphene-DNA functional structures.

Analyte	Detection strategy	Sensing interface	Detection mode	LOD	Ref.
ATP	FAM-labeled aptamer	GO	Fluorescence anisotropy	1×10^{-7} M	227
	Upconversion nanophosphors labeled aptamer,	GO	Fluorescence	8×10^{-8} M,	228
	Molecular aptamer beacon,			2×10^{-6} M,	229
	FAM labeled aptamer,			4.5×10^{-7} M,	339
	ATP-dependent enzymatic reaction			3×10^{-10} M	340
	Triplex DNA amplification	Graphene/mesoporous silica/GNPs	Electrochemical	2.3×10^{-11} M	231
	Ferrocene-labeled aptamers	Magnetic graphene nanosheets	Electrochemical	1×10^{-10} M	341
	Label free ATP aptamer	Porphyrin/graphene	Electrochemical	7×10^{-10} M	230

		hybrid nanosheets			
	Aptamer-SiO_2 nanospheres/graphene QDs	Au electrode	Electrochemilum inescence	1.5×10^{-12} M	[342]
Cocaine	Streptavidin-conjugated alkaline phosphatases	Aptamer/graphene/GNPs hybrid	Electrochemical	1×10^{-9} M	[202]
	Aptamer labeled with GNPs	Aptamer-functionalized GO	Fluorescence	1×10^{-7} M	[234]
Glucose	Direct electrochemistry and electrocatalysis	GOx/DNA/graphene hybrid	Electrochemical	3×10^{-7} M	[249]
Dopamine	Dopamine aptamer	Graphene–polyaniline composite	Electrochemical	1.98×10^{-12} M	[248]
	Graphene/ssDNA interaction	Thiol-ssDNA modified Au electrode	Electrochemical	8×10^{-10} M	[343]

Cysteine	Thiol-activated DNA metallization, chelation between Ag ions and G-rich FAM-ssDNA, competitive ligation of Hg^{2+} with T–T mismatches	GO	Fluorescence	2×10^{-9} M, 1×10^{-7} M, 2×10^{-9} M	344, 242, 345
L-histidine	L -histidine-dependent DNAzyme	Au NPs-graphene nanosheets	Electrochemical	1×10^{-13} M	250
Biotin	Ligation between biotin and streptavidin	Streptavidin–DNA conjugate/GO	Fluorescence	4.4×10^{-10} M	244
Nonylphenol	Differential pulse voltammetry	Graphene–DNA/glassy carbon electrode	Electrochemical	1×10^{-8} M	346
Coralyne	Participating interaction into the aptamer duplex	GO	Fluorescence	1×10^{-8} M	230
Theophylline	Self-cleaving RNA ribozyme with endonuclease	GO	Fluorescence	1×10^{-7} M	246
D-vasopressin	Layer-by-layer assembly	Polyelectrolyte-methylene blue/polyelectrolyte-graphen	Electrochemical	1 ng/mL	347

		e			
Ochratoxin A	Upconversion fluorescent nanoparticles labeled aptamer	GO	Fluorescence	0.02 ng/mL	[238]
Bleomycin	Irreversible cleavage with bleomycin and Fe(II)	GO -ssDNA complex	Fluorescence	2×10^{-10} M	[247]

Table 2. Comparison of different thrombin biosensors by using graphene and functional DNA structures.[a]

Technique	Detection strategy	Sensing interface	LOD (M)	Ref.
EC	Aptamer recognition	Graphene-aptamer covalent conjugate	4.5×10^{-16}	241
		Nickel hexacyanoferrate nanoparticles/nafion graphene composites	3×10^{-13}	348
		Au NPs/thionine–graphene nanocomposite	9.3×10^{-11}	252
		Au NPs-polyaniline-graphene united GOD-MPTS biocomposite	5.6×10^{-13}	254
		Orange II functionalized graphene nanosheets	3.5×10^{-13}	253
		Aptamer/methylene blue-anchored GO	3.05×10^{-12}	349
	Sandwich-type aptasensor	**Sensing interface**	**Secondary label**	
		CS-HCoPt- Aptamer I	HCoPt-reduced GO-Thi-HRP-Aptamer II	3.4×10^{-13} 258

		GO-Aptamer I *via* covalent bond	ALP-Au-Aptamer II	2.7×10^{-15}	257
		Au NPs/PATP/avidin-biotin Aptamer I	Hemin/G-quadruplex/toluidine blue/graphene-Pd NPs composites-Aptamer II	3×10^{-14}	238
		PAMAM–CNTs-Aptamer I	GOD–Pt NPs@reduced GO-Aptamer II	2.1×10^{-13}	235
		Au NPs-thionine-Aptamer I	Hemin/G-quadruplex/thionine-PAMAM- reduced GO-Aptamer II	1×10^{-13}	350
ECL	Hybridization between Fc-MB and capture DNA	Graphene-CNT/Nafion/ $Ru(bpy)_3^{2+}$-Pt NPs		1.7×10^{-12}	330
	Hybridization between	Aptamer covalently binding graphene		4×10^{-13}	255

	aptamer and its complementary part inserted with $Ru(bpy)_3^{2+}$			
ECL	DNA cycle amplification with magnetic microbeads-bound CdS NPs	Mercaptoethylamine assembly bound with GO	1×10^{-15}	351
	Sandwich-type aptasensor	GO/PEI–PTCDA-glutaraldehyde-aptamer II; electrodeposition of Au monolayer- Aptamer I	3.3×10^{-16}	260
FL	FAM labeled aptamer	Sodium dodecyl benzene sulfonate-graphene	3.13×10^{-11}	107
UV–vis	Distance-dependent optical properties	Monodispersed aptamer functionalized GNPs	5×10^{-12}	264

FET	Bio-recognition PBASE–aptamer	Large-area chemical vapor deposition derived graphene	1×10^{-7}	197
SPR	Aptamer recognition	Chemical reduction of GO assembled on a positively charged SPR Au (p-Au) film	3×10^{-11}	266
CL	Chemiluminescence resonance energy transfer from luminol-H_2O_2-HRP to FAM	FAM labeled probe DNA–GO complex	1×10^{-13}	263
Microscope	Aptamer recognition	Aptamer/pyrene linker/single GO piece fixed on a Si/SiO_2 solid support	n/a	265

[a] EC, electrochemical; ECL, electochemiluminescence; FL, fluorecence; FET, field-effect transistor; SPR, surface plasmon resonance; CL, chemiluminescence; GOD, glucose oxidase; MPTS, (3-mercaptopropyl)trimethoxysilane; CS, chitosan; HCoPt, hollow CoPt bimetal alloy nanoparticles; Thi, thionine; HRP, horseradish peroxidase; ALP, alkaline phosphatase; PATP, p-aminothiophenol; PAMAM, poly(amino–amine) dendrimers; Fc, ferrocene; PTCDA, 3,4,9,10- perylenetetracarboxylic dianhydride; PBASE, pyrenebutanoic acid succin-imidyl ester; FAM,

carboxyfluorescein.

Table 3. Table of the various gene delivery systems by using graphene and DNA.[a]

Cargo	Vector	Cell	Target	Ref.
Plasmid DNA	GO chemically-functionalized with branched PEI	HeLa cells	GFP and luciferase reporter	352
siRNA	PEGylated PEI-grafted graphene/Au composites	Human promyelocytic leukemia cells	Bcl-2 protein	353
Locked nucleic acid modified molecular beacon probe	PEI-grafted graphene nanoribbon	HeLa cells	miRNA(miR-21)	327
Small interfering RNA	PEG and PEI covalently conjugated nano GO	HeLa cells	Polo-like kinucleic acidse 1 (Plk1)	325
Plasmid DNA	GO-PEI (1.2 k) and GO-PEI (10 k)	HeLa cells	GFP	326
Plasmid DNA	Branched PEI-GO hybrid	HeLa cells and human prostate cancer cells	Luciferase reporter	354, 21

FAM labeled multifunctional DNAzyme	Nano-sized GO	Human liver cells	Hepatitis C virus mRNA [332]
NLS peptide PKKKRKV	Engineered PEI/GO nanocomposite	293 T cells	Nuclear localized signals [331]
GFP-specific siRNA	Linear PEI-grafted GO	HEK293 cells	GFP [355]
Enhanced GFP plasmid reporter gene	PEI grafted ultra-small GO	H293T cells and U2Os cells	GFP [333]

[a] GFP, green fluorescent protein; PEI, polyethylenimine; PEG, polyethylene glycol.

Scheme 1. Schematically illustration of the biotechnological applications of graphene and nucleic acids nanobiointerface.

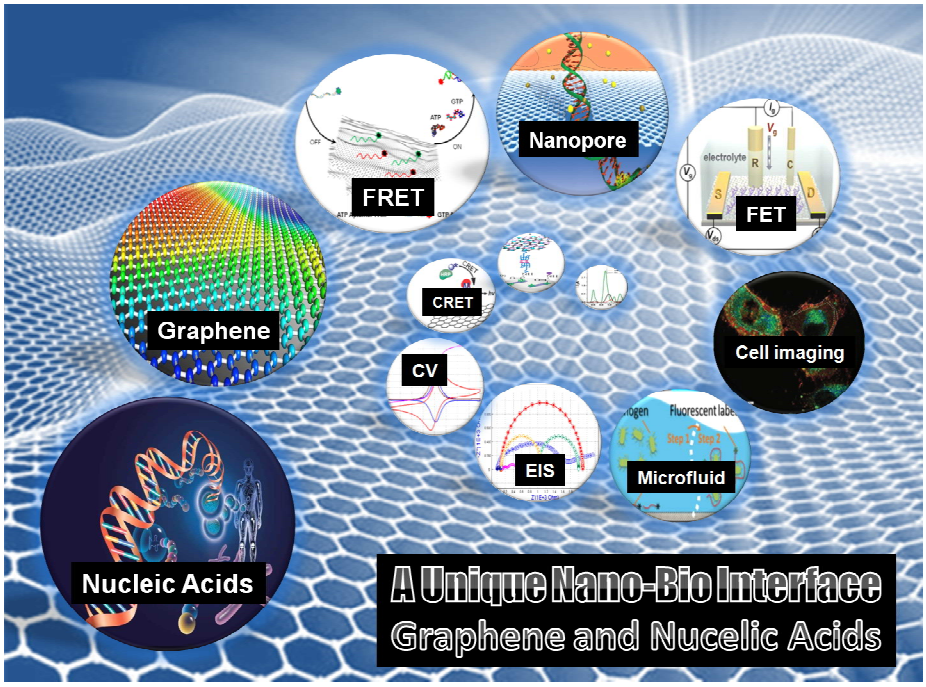

Figure 1. DPVs at a GC (A), graphite/GC (B) and chemical reduced (CR) GO/GC electrode (C) for nucleobases. (D) DPVs for a mixture of G, A, T, and C at CR-GO/GC, graphite/GC, and GC electrodes. (E) DPVs for ssDNA at CR-GO/GC (green), graphite/GC (red), and GC electrodes (black). (F) DPVs for dsDNA at CR-GO/GC (green), graphite/GC (red), and GC electrodes (black). (Reproduced with permission from ref. 177)

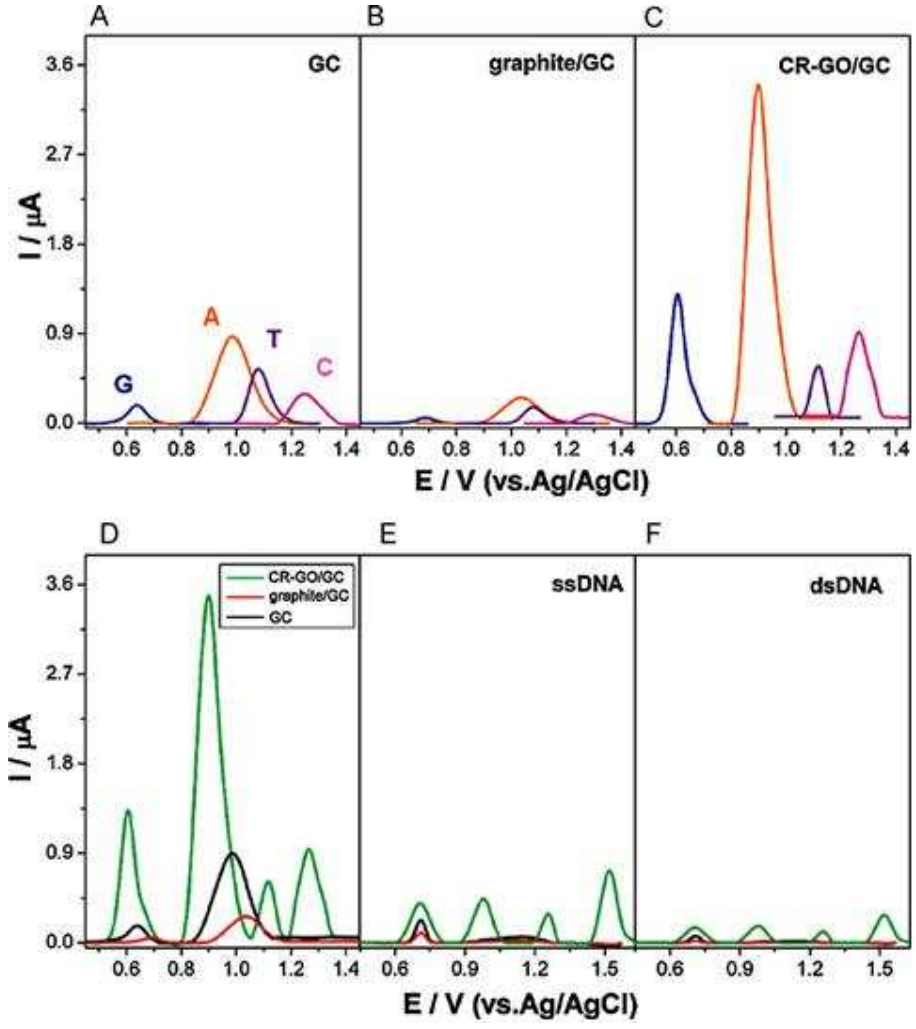

Figure 2 The dsDNA translocation through graphene nanopores. Illustration and/or data from (A) Dekker lab;[206] (B) Golovchenko lab;[209] (C) Drndić lab;[208] and (D) Bashir lab[210].(Reproduced with permission from ref. 206, 208, 209 and 210)

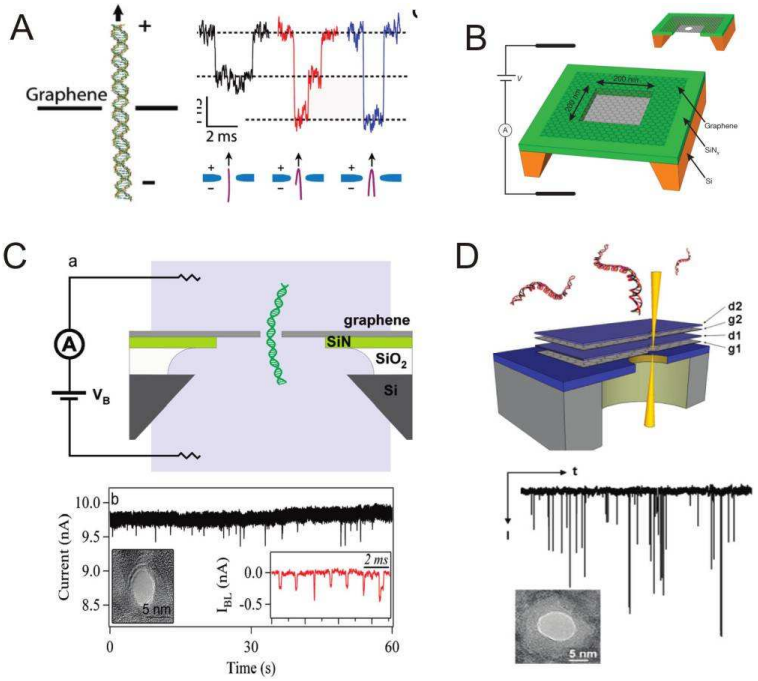

Figure 3. (A) Schematic illustration of the upconversion fluorescence resonance energy transfer between ssDNA- upconversion nanophosphors (UCNPs) and GO for ATP sensing.[228] (B) The secondary structure of the D -VP binding 55-mer DNA aptamer, the aptamer 21-mer and 34-mer DNA. The specific D-vasopressin enantiomer binding sites is the asymmetric internal loop of 20-mer nucleotides (Loop1). Schematic representation of the sensing procedure for the analysis of D-VP based on the sensing platform with graphene–mesoporous silica–gold nanoparticle hybrids (GSGHs) as enhanced materials and Fc-PEI as electrochemical probe.[237] (Reproduced with permission from ref. 228 and ref. 237)

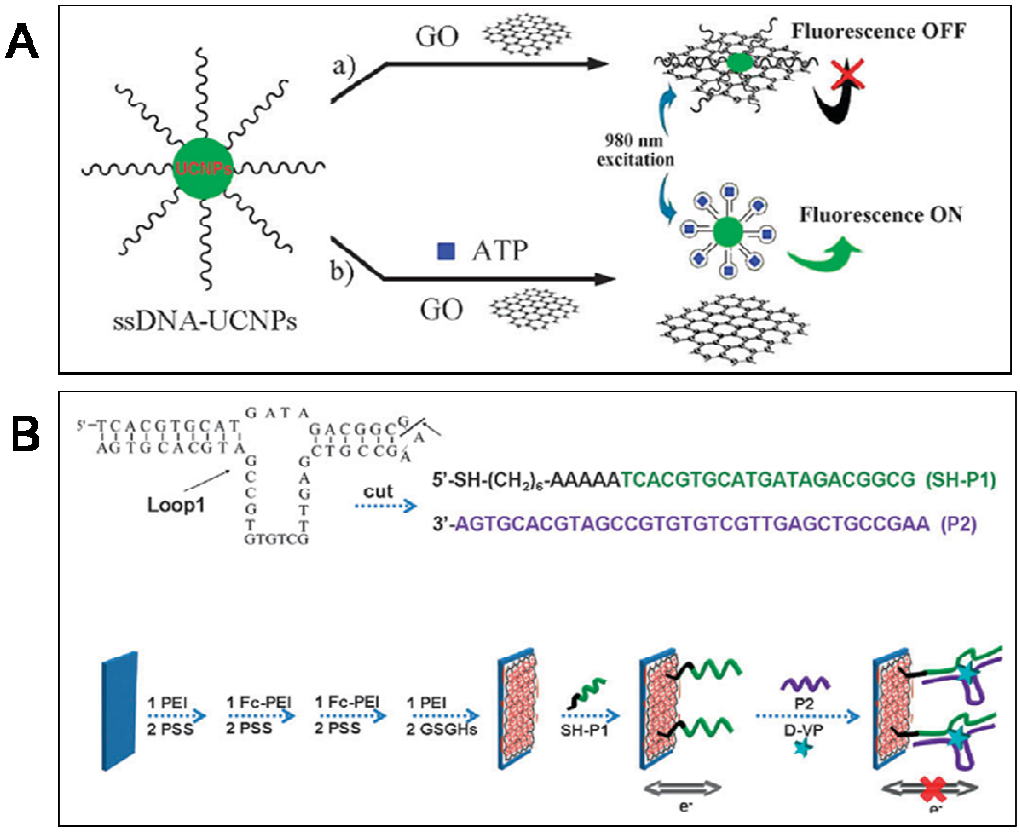

Figure 4. Illustration of the sandwich type electrochemical aptasensor for thrombin detection based on poly (amino–amine) dendrimers (PMMA)–CNTs as platform and aptamer-glucose oxidase-PtNPs@reduced GO bio-conjugate for signal response and amplification. (Reproduced with permission from ref. 256)

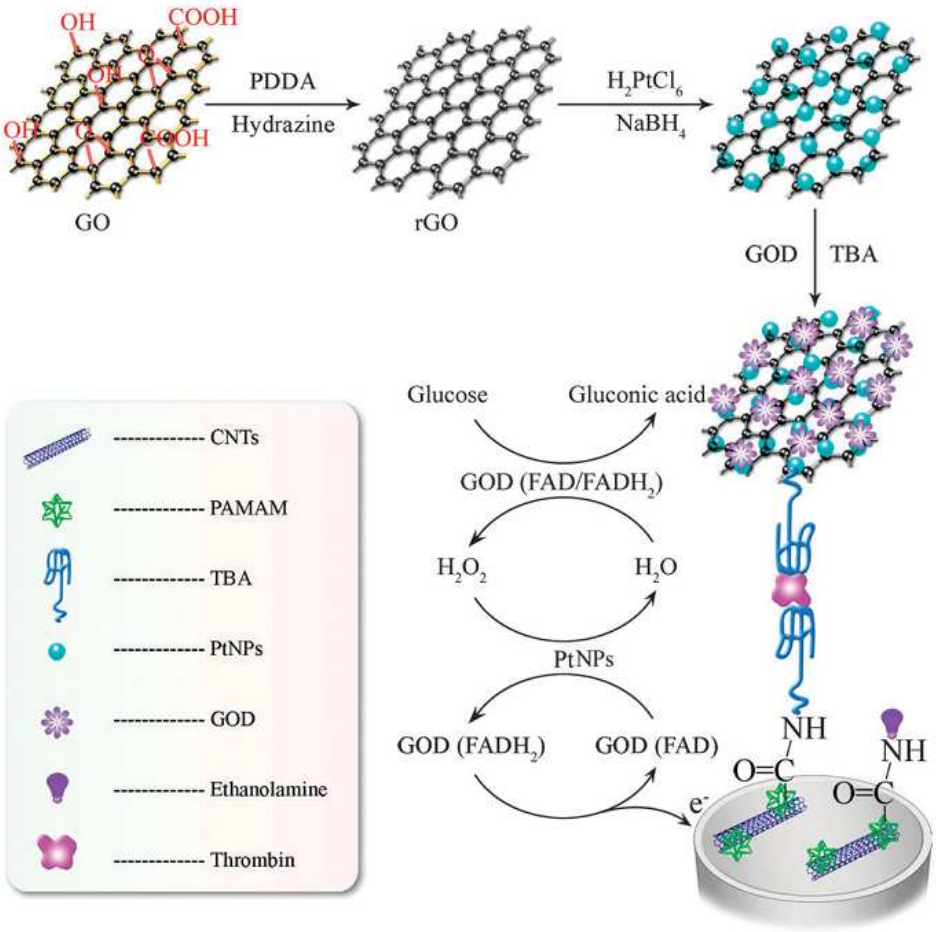

Figure 5. (A) Schematic illustration of target DNA induced chemiluminescence resonance energy transfer (CRET) change of the FAM labeled probe DNA–GO complex.[263] (B) Schematic demonstration of SDBS-graphene FRET aptasensor and the detection mechanism for thrombin.[107] (Reproduced with permission from ref.263 and ref. 107)

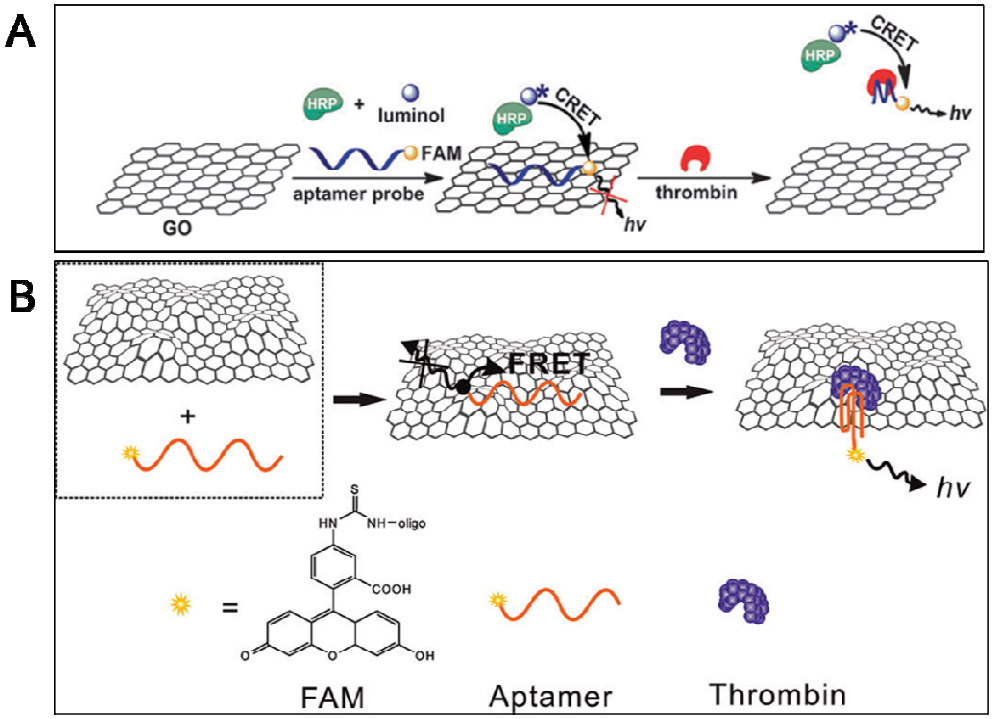

Figure 6. (A) Synthetic protocol of polypyrrole-converted nitrogen-doped few-layer graphene (PPy-NDFLG) on flexible substrate. (B) (a) Current voltage curves of PPy-NDFLG on the PEN film before and after aptamer immobilization in air (V_{ds}= -0.5 V to +0.5 V and scan rate was 10 mV s^{-1}). (b) Schematic diagram of a liquid-ion gated FET using aptamer-conjugated PPy-NDFLG (Ag/AgCl reference electrode, R; platinum counter electrode, C; source and drain electrodes, S and D). (c) I_{ds}-V_{ds} output characteristics of PPy-NDFLG-aptamer at different V_g from -0.1 to 0.5 V in a step of 0.1 V in phosphate-buffered solution (V_{ds}, 0 to 0.5V in a step of 50 mV). (d) Real-time responses and a calibration curve (S in the inset indicates $\Delta I/ I_0$) of aptasensor with various vascular endothelial growth factor concentrations. (Reproduced with permission from ref. 270

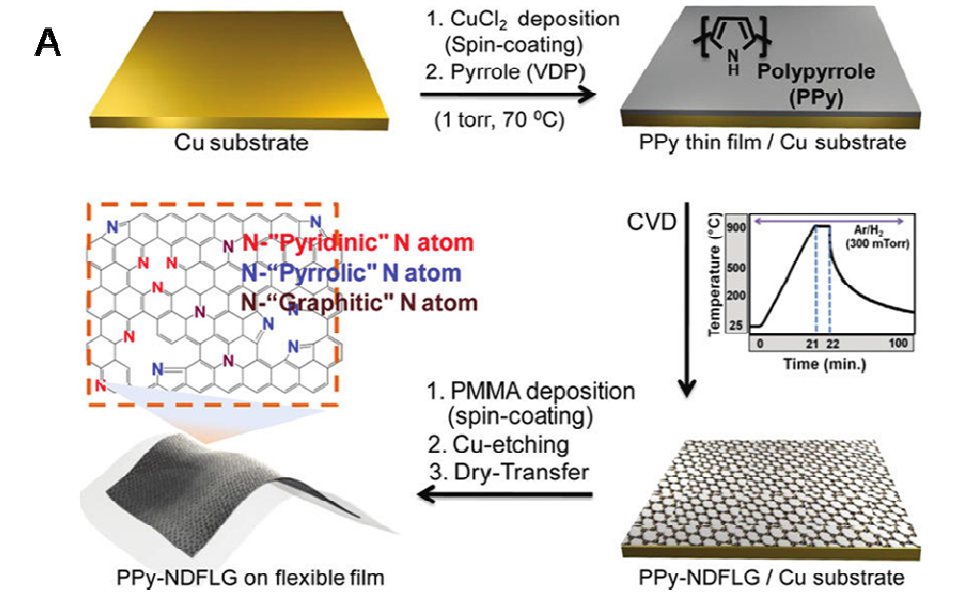
A
1. $CuCl_2$ deposition
(Spin-coating)
2. Pyrrole (VDP)
(1 torr, 70 °C)
Cu substrate
Polypyrrole
(PPy)
PPy thin film / Cu substrate
CVD
Temperature (°C)
900
500
200
25
Ar/H2
(300 mTorr)
0
21
22
100
Time (min.)
N-"Pyridinic" N atom
N-"Pyrrolic" N atom
N-"Graphitic" N atom
1. PMMA deposition
(spin-coating)
2. Cu-etching
3. Dry-Transfer
PPy-NDFLG on flexible film
PPy-NDFLG / Cu substrate

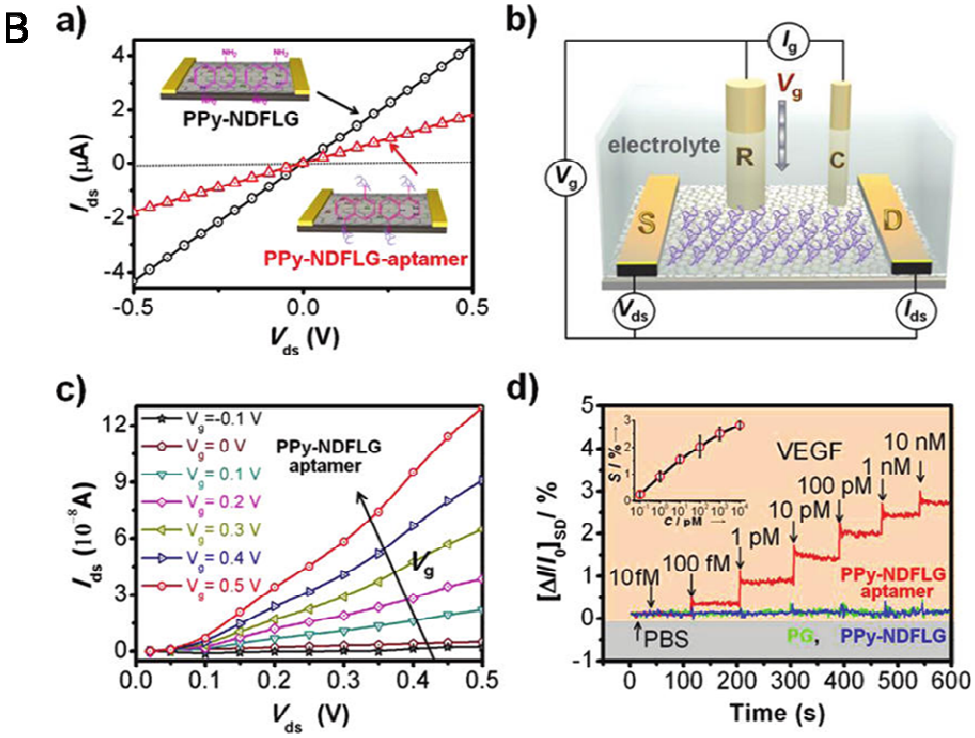
B
a)
PPy-NDFLG
PPy-NDFLG-aptamer
I_{ds} (μA)
V_{ds} (V)
b)
I_g
V_g
electrolyte
R
C
S
D
V_{ds}
I_{ds}
c)
V_g =-0.1 V
V_g = 0 V
V_g = 0.1 V
V_g = 0.2 V
V_g = 0.3 V
V_g = 0.4 V
V_g = 0.5 V
PPy-NDFLG
aptamer
I_{ds} (10^{-8} A)
V_{ds} (V)
d)
S / %
c / pM
VEGF
10 nM
1 nM
100 pM
10 pM
1 pM
100 fM
10fM
PPy-NDFLG
aptamer
PBS
PG, PPy-NDFLG
$[\Delta I/I_0]_{SD}$ / %
Time (s)

Figure 7. Nyquist plot before (blue solid square) and after (red solid triangle) DNA-probe immobilization by (a) covalent grafting and (b) π–π stacking; incubating the electrodes in a hybridization buffer containing different concentrations of DNA-target for 40 min at 42 °C: (a) 50 fM, 1 pM, 50 pM, 1 nM, 50 nM, and 1μM and (b) 1 fM, 50 fM, 1 pM, 50 pM, and 1 nM. Inset: Plot of Δ Rct against the concentration of DNA-target and equivalent circuit modeling. Corresponding admittance plot for (c) covalent grafting or (d) π-π stacking plot before (blue solid square) and after DNA-probe immobilization (red solid triangle), after incubation in the presence of a single base mismatch DNA solution (solid green triangle) or cDNA-target (solid black curve) 1 nM and after denaturation (open square). (Reproduced with permission from ref. 184)

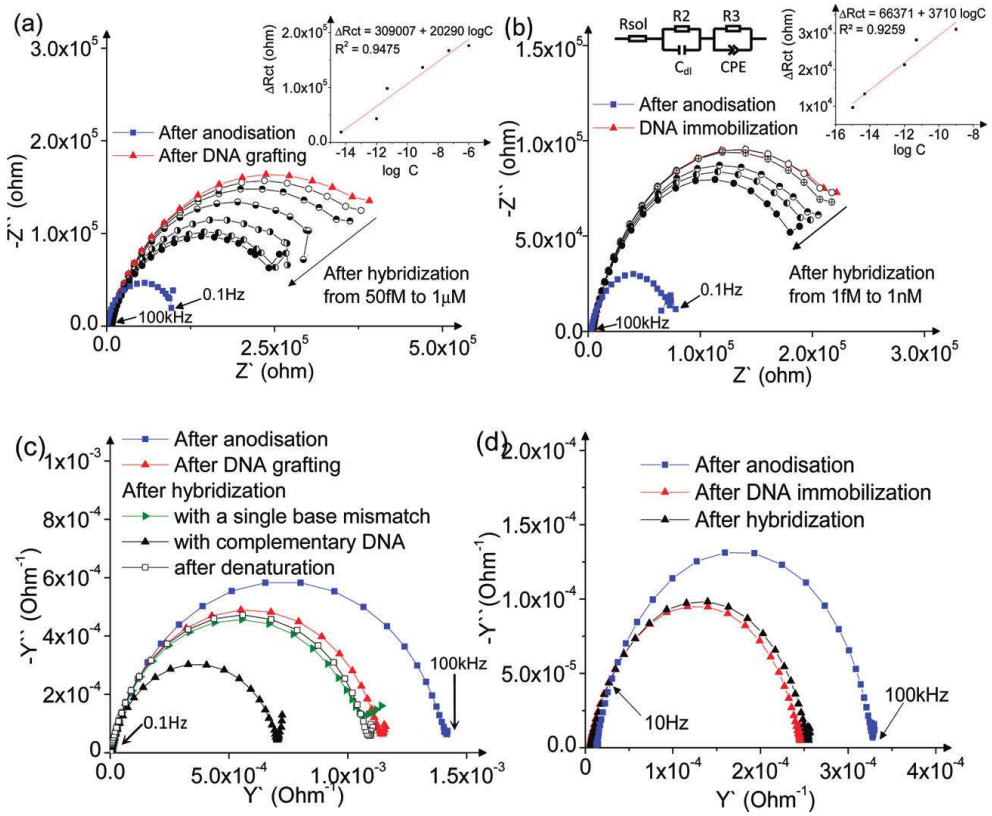

Figure 8. Schematic of the PDMS/paper hybrid microfluidic system for one-step multiplexed pathogen detection using aptamer-functionalized GO biosensors (not drawn to scale). (a) Microfluidic biochip layout, (b) and (c) illustrate the principle of the one-step 'turn-on' detection approach based on the interaction among GO, aptamers and pathogens. Step 1: when an aptamer is adsorbed on the GO surface, its fluorescence is quenched. Step 2: when the target pathogen is present, the target pathogen induces the aptamer to be liberated from GO and thereby restores its fluorescence for detection. (Reproduced with permission from ref. 318)

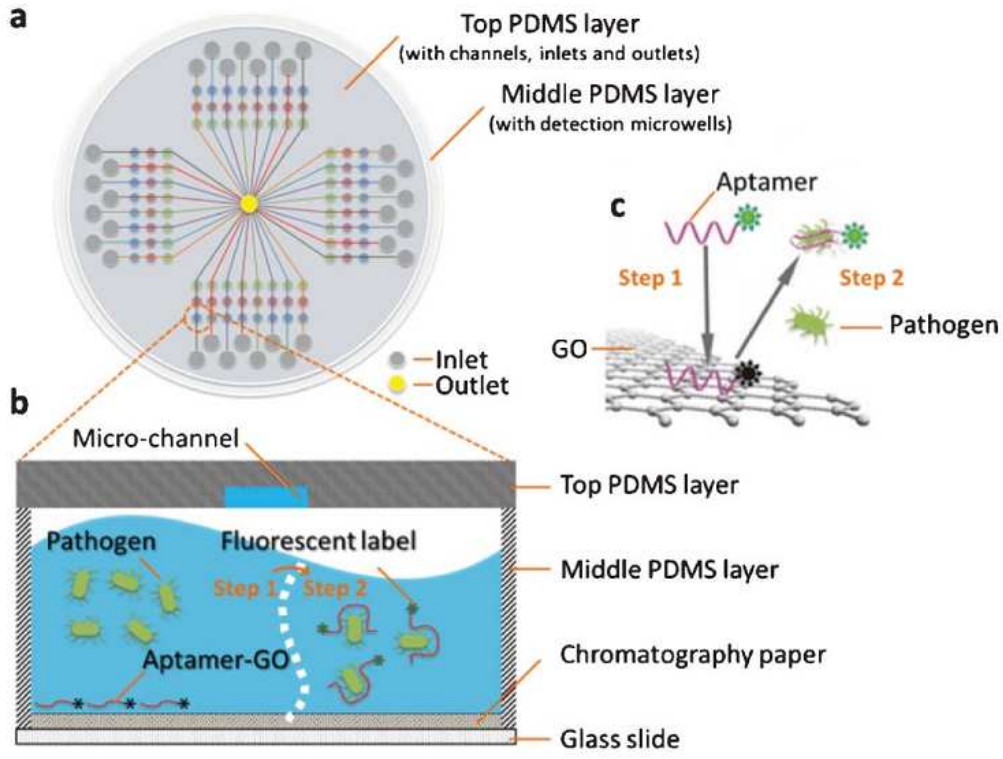

Figure 9. (A) Binding of ATP aptamer-FAM and GTP aptamer-Cy5 to GO-nS led to fluorescence off due to the FRET effect between fluorophores and GO-nS. After incorporating the analytes (ATP or GTP), loop-structured assemblies of aptamer-ATP and aptamer-GTP were released from GO-nS and resulted in fluorescence on. *In situ* simultaneous probing of ATP and GTP in living cells was realized consequently by using this fluorescence off/on switch concept.[134] (B) Fluorescence images of Huh-7-rep cells that were treated with FAM-Dz/nGO and FAM-scDz/nGO (1.0m M) for 12 h. Fluorescence of FAM was turned on only when the Dz complementary to target HCV NS3 RNA was used. Blue: nucleus stained with Hoechst 33342, green: FAM.[334] (Reproduced with permission from ref. 134 and ref. 334)

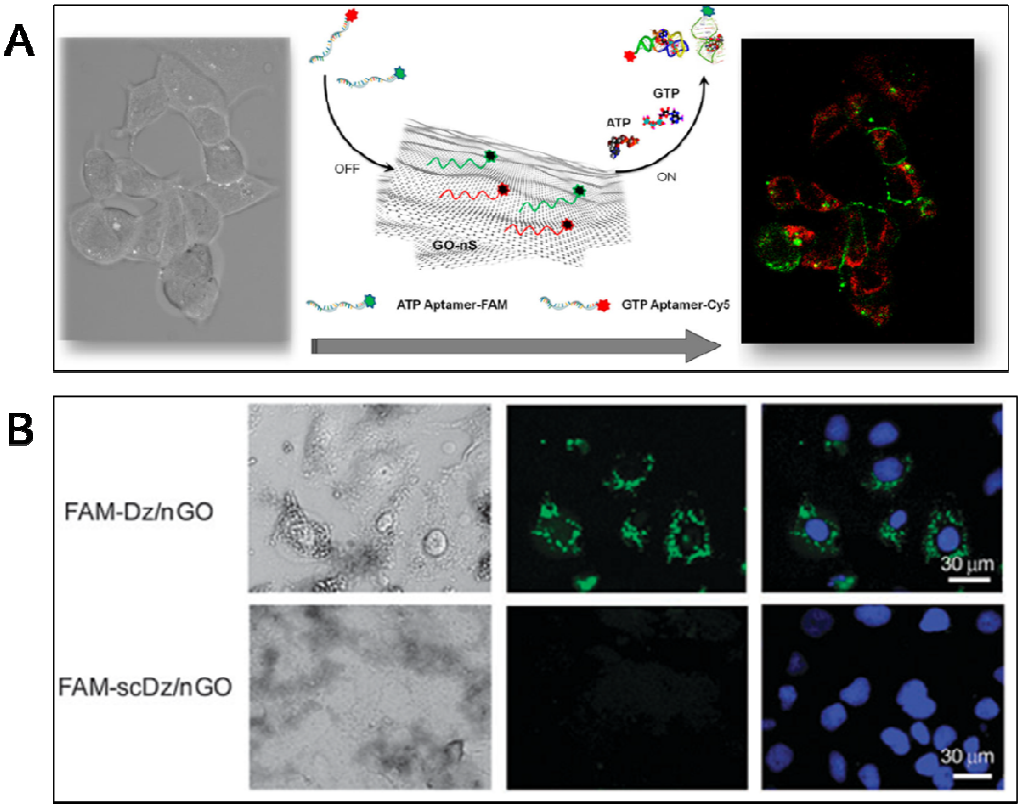

Reference

1. L. Shang, G. U. Nienhaus, *Mater. Today*, **2013**, ***16***, 58-66.
2. L. H. Tang, H. Chang,Y. Liu, J. Li, *Adv. Funct. Mater.*, 2012, **22**, 3083-3088.
3. A. M. Alkilany, S. E. Lohse, C. J. Murphy, *Accounts Chem. Res.*, 2012, **46**, 650-661.
4. D. F. NguyenMoyano, V. M. Rotello, *Langmuir*, 2011, **27**, 10376-10385.
5. A. E. Nel, L. Mädler, D. Velegol, T. Xia, E. M. Hoek, P. Somasundaran, F. Klaessig, V. Castranova, M. Thompson, *Nat. Mater.*, 2009, **8**, 543-557.
6. T. O. Yeates, *Nat. Nanotechnol.* 2011, **6**, 541-542
7. N. L. Rosi and C. A. Mirkin, *Chem. Rev.*, 2005, **105**, 1547-1562.
8. D. J. Maxwell, J. R. Taylor and S. Nie, *J. Am. Chem. Soc.*, 2002, **124**, 9606-9612.
9. K. Shoorideh, C. O. Chui, *Proc. Natl. Acad. Sci. U.S.A.* 2014, **111**, 5111-5116
10. C. A. Mirkin and C. M. Niemeyer, Nanobiotechnology II: More Concepts, Applications, *Wiley-VCH*, *Wiley-VCH,* Germany, 2007
11. D. Gebauer, *Angew. Chem. Int. Edit.*, 2013, **52**, 8208-8209.
12. H. J. Tang, C. M. Hessel, J. Y. Wang, N. L. Yang, R. B. Yu, H. J. Zhao and D. Wang, *Chem. Soc. Rev.*, 2014, **43**, 4281-4299.
13. P. Nguyen and V. Berry, *J. Phys. Chem. Lett.*, 2012, **3**, 1024-1029.
14. C. A. Mirkin, R. L. Letsinger, R. C. Mucic and J. J. Storhoff, *Nature*, 1996, **382**, 607-609.
15. A. P. Alivisatos, K. P. Johnsson, X. Peng, T. E. Wilson, C. J. Loweth, M. P. Bruchez and P. G. Schultz, *Nature,* 1996, **382**, 609-611
16. J. Chen and N. C. Seeman, *Nature*, 1991, **350**, 631-633.
17. J. H. Chen, N. R. Kallenbach and N. C. Seeman, *J. Am. Chem. Soc.*, 1989, **111**, 6402-6407.
18. C. Murray, D. J. Norris and M. G. Bawendi, *J. Am. Chem. Soc.*, 1993, **115**, 8706-8715.
19. X. Peng, L. Manna, W. Yang, J. Wickham, E. Scher, A. Kadavanich and A. P. Alivisatos, *Nature*, 2000, **404**, 59-61.
20. M. Bruchez, M. Moronne, P. Gin, S. Weiss and A. P. Alivisatos, *Science*, 1998, **281**, 2013-2016.
21. W. C. Chan and S. Nie, *Science*, 1998, **281**, 2016-2018.
22. Q. A. Pankhurst, J. Connolly, S. Jones and J. Dobson, *J . Phys. D: Appl. Phys.*, 2003, **36**, R167.
23. Y.-w. Jun, Y.-M. Huh, J.-s. Choi, J.-H. Lee, H.-T. Song, S. Kim, S. Kim, S. Yoon, K.-S. Kim and J.-S. Shin, *J. Am. Chem. Soc.*, 2005, **127**, 5732-5733.
24. R. Weissleder, A. Moore, U. Mahmood, R. Bhorade, H. Benveniste, E. A. Chiocca and J. P. Basilion, *Nat. Med.*, 2000, **6**, 351-354.
25. S. Iijima, *Nature*, 1991, **354**, 56-58.
26. X. Duan and C. M. Lieber, *J. Am. Chem. Soc.*, 2000, **122**, 188-189.
27. A. M. Morales and C. M. Lieber, *Science*, 1998, **279**, 208-211.
28. T. J. Trentler, K. M. Hickman, S. C. Goel, A. M. Viano, P. C. Gibbons and W. E. Buhro, *Science*, 1995, **270**, 1791-1794.

29. E. Katz and I. Willner, *Chemphyschem*, 2004, **5**, 1084-1104.
30. M. Shim, N. W. Shi Kam, R. J. Chen, Y. Li and H. Dai, *Nano Lett.*, 2002, **2**, 285-288.
31. Y. Cui, Q. Wei, H. Park and C. M. Lieber, *Science*, 2001, **293**, 1289-1292.
32. K. Besteman, J.-O. Lee, F. G. Wiertz, H. A. Heering and C. Dekker, *Nano Lett.*, 2003, **3**, 727-730.
33. K. S. Novoselov, A. K. Geim, S. V. Morozov, D. Jiang, Y. Zhang, S. V. Dubonos, I. V. Grigorieva and A. A. Firsov, *Science*, 2004, **306**, 666-669.
34. S. V. Morozov, K. S. Novoselov, A. K. Geim, *Phys.-Usp.*, 2008, **51**, 744-748.
35. D. Chen, H. Feng and J. Li, *Chem. Rev.*, 2012, **112**, 6027-6053.
36. D. Chen, L. Tang and J. Li, *Chem. Soc. Rev.*, 2010, **39**, 3157-3180.
37. D. R. Dreyer, S. Park, C. W. Bielawski and R. S. Ruoff, *Chem. Soc. Rev.*, 2010, **39**, 228-240.
38. A. K. Geim and K. S. Novoselov, *Nat. Mater.*, 2007, **6**, 183-191.
39. K. S. Novoselov, A. K. Geim, S. V. Morozov, D. Jiang, M. I. Katsnelson, I. V. Grigorieva, S. V. Dubonos, A. A. Firsov, *Nature* 2005, **438**, 197-200.
40. L. Z. Feng and Z. A. Liu, *Nanomedicine*, 2011, **6**, 317-324.
41. M. Pumera, *Mater. Today*, 2011, **14**, 308-315.
42. J. P. Li, Y. Zhang, J. K. Yang, K. D. Bi, Z. H. Ni, D. Y. Li and Y. F. Chen, *Phys. Rev. E*, 2013, **87**.
43. B. M. Venkatesan and R. Bashir, *Nat. Nanotechnol.*, 2011, **6**, 615-624.
44. J. W. Liu, *Phys. Chem. Chem. Phys.*, 2012, **14**, 10485-10496
45. Z. B. Liu, B. W. Liu, J. S. Ding, J. W. Liu, *Anal. Bioanal. Chem.*, 2014, **406**, 6885-6902
46. D. Li, S. P. Song and C. H. Fan, *Acc. Chem. Res.*, 2010, **43**, 631-641.
47.C. Hong, D. M. Kim, A. Baek, H. Chung, W. Jung and D. E. Kim, *Chem Commun*, 2015, **51**, 5641-5644.
48. S. P. Song, Y. Qin, Y. He, Q. Huang, C. H. Fan and H. Y. Chen, *Chem. Soc. Rev.*, 2010, **39**, 4234-4243.
49. Y. Jalit, M. Moreno, F. A. Gutierrez, A. S. Arribas, M. Chicharro, E. Bermejo, A. Zapardiel, C. Parrado, G. A. Rivas and M. C. Rodriguez, *Electroanal.*, 2013, **25**, 1116-1121.
50. S. Navalon, A. Dhakshinamoorthy, M. Alvaro, and H. Garcia, *Chem. Rev.* 2014, 114, 6179−6212
51. J. D. Roy-Mayhew, and I. A. Aksay, *Chem. Rev.* 2014, 114, 6323−6348
52. M. M. Liu, R. Z. Zhang, and W. Chen, *Chem. Rev.* 2014, 114, 5117−5160
53. Y. Wang, Z. H. Li, J. Wang, J. H. Li and Y. H. Lin, *Trends Biotechnol.*, 2011, **29**, 205-212.
54. H. J. Jiang, *Small,* 2011, **7**, 2413-2427
55. D. Du, Y. Q. Yang and Y. H. Lin, *MRS Bull*, 2012, **37**, 1290-1296.
56. T. Kuila, S. Bose, P. Khanra, A. K. Mishra, N. H. Kim and J. H. Lee, *Biosens. Bioelectron.*, 2011, **26**, 4637-4648.
57. Wu, L.; Wang, J. S.; Ren, J. S.; Qu, X. G. *Adv.Funct. Mater.,* **2014**, *24*, 2727.
58. Xing, X. J.; Zhou, Y.; Liu, X. G.; Pang, D. W.; Tang, H. W. *Small* **2014**, *10*, 3412.

59. Liu, M.; Song, J. P.; Shuang, S. M.; Dong, C.; Brennan, J. D.; Li, Y. F. *ACS Nano* **2014**, *8*, 5564.
60. J. C. Meyer, A. K. Geim, M. Katsnelson, K. Novoselov, T. Booth and S. Roth, *Nature*, 2007, **446**, 60-63.
61. C. N. R. Rao and A. K. Sood, Graphene: Synthesis, Properties, and Phenomena, *John Wiley & Sons*, 2013.
62. P. Avouris and C. Dimitrakopoulos, *Mater. Today*, 2012, **15**, 86-97.
63. X. Li, W. Cai, J. An, S. Kim, J. Nah, D. Yang, R. Piner, A. Velamakanni, I. Jung, E. Tutuc, S. K. Banerjee, L. Colombo and R. S. Ruoff, *Science*, 2009, **324**, 1312-1314.
64. J. Coraux, A. T. N`Diaye, C. Busse and T. Michely, *Nano Lett.*, 2008, **8**, 565-570.
65. S. Chen, W. Cai, R. D. Piner, J. W. Suk, Y. Wu, Y. Ren, J. Kang and R. S. Ruoff, *Nano Lett.*, 2011, **11**, 3519-3525.
66. S. Park and R. S. Ruoff, *Nat. Nanotechnol.*, 2009, **4**, 217-224.
67. O. Akhavan, E. Ghaderi and H. Emamy, *J. Mater. Chem.*, 2012, **22**, 20626-20633.
68. A. Walcarius, S. D. Minteer, J. Wang, Y. H. Lin and A. Merkoci, *J. Mat. Chem. B*, 2013, **1**, 4878-4908.
69. L. M. Zhang, Z. X. Lu, Q. H. Zhao, J. Huang, H. Shen and Z. J. Zhang, *Small*, 2011, **7**, 460-464.
70. H. Q. Bao, Y. Z. Pan, Y. Ping, N. G. Sahoo, T. F. Wu, L. Li, J. Li and L. H. Gan, *Small*, 2011, **7**, 1569-1578.
71. C. Wang, C. Y. Wu, X. J. Zhou, T. Han, X. Z. Xin, J. Y. Wu, J. Y. Zhang and S. W. Guo, *Sci. Rep.*, 2013, **3**., 2013, 3, 2852-2859.
72. Z. Liu, J. T. Robinson, S. M. Tabakman, K. Yang and H. J. Dai, *Mater. Today*, 2011, **14**, 316-323.
73. Y. Wang, Z. H. Li, D. H. Hu, C. T. Lin, J. H. Li and Y. H. Lin, *J. Am. Chem. Soc.*, 2010, **132**, 9274-9276.
74. Z. Liu, J. T. Robinson, X. M. Sun and H. J. Dai, *J. Am. Chem. Soc.*, 2008, **130**, 10876-10877.
75. X. Chen, X. J. Zhou, T. Han, J. Y. Wu, J. Y. Zhang and S. W. Guo, *ACS Nano*, 2013, **7**, 531-537.
76. A. He, B. Lei, C. Cheng, S. Li, L. Ma, S. D. Sun and C. S. Zhao, *RSC Adv.*, 2013, **3**, 22120-22129.
77. J. S. Park, A. Baek, I. S. Park, B. H. Jun and D. E. Kim, *Chem. Commun.*, 2013, **49**, 9203-9205.
78. K. Hu, J. W. Liu, J. Chen, Y. Huang, S. L. Zhao, J. N. Tian and G. H. Zhang, *Biosens. Bioelectron.*, 2013, **42**, 598-602.
79. X. R. Zhang, Y. P. Xu, Y. Q. Yang, X. Jin, S. J. Ye, S. S. Zhang and L. L. Jiang, *Chem. Eur. J.*, 2012, **18**, 16411-16418.
80. E. Chargaff, The Nucleic Acids, *Elsevier*, 2012.
81. J. Liu, Z. Cao and Y. Lu, *Chem. Rev.*, 2009, **109**, 1948-1998.
82. D. Shangguan, Y. Li, Z. Tang, Z. C. Cao, H. W. Chen, P. Mallikaratchy, K. Sefah, C. J. Yang and W. Tan, *Proc. Natl. Acad. Sci. U.S.A.*, 2006, **103**, 11838-11843.
83. Q. Yuan, D. Q. Lu, X. B. Zhang, Z. Chen and W. H. Tan, *TrAC-Trends Anal. Chem.*, 2012, **39**, 72-86.

84. M. Famulok and G. Mayer, *Acc.Chem. Res.*, 2011, **44**, 1349-1358.
85. A. B. Iliuk, L. Hu and W. A. Tao, *Anal. Chem.*, 2011, **83**, 4440-4452.
86. W. Tan, K. Wang and T. J. Drake, *Curr. Opin. Chem. Biol.*, 2004, **8**, 547-553.
87. R. Vansweevelt, A. Malesevic, M. Van Gompel, A. Vanhulsel, S. Wenmackers, J. D'Haen, V. Vermeeren, M. Ameloot, L. Michiels, C. Van Haesendonck and P. Wagner, *Chem. Phys. Lett.*, 200, **485**, 196-201.
88. S. Liu and X. F. Guo, *NPG Asia Mat.*, 2012, **4**, 1-10.
89. A. Nunes, N. Amsharov, C. Guo, J. Van den Bossche, P. Santhosh, T. K. Karachalios, S. F. Nitodas, M. Burghard, K. Kostarelos and K. T. Al-Jamal, *Small*, 2010, **6**, 2281-2291.
90.H. L. Li, Y. W. Zhang, Y. L. Luo and X. P. Sun, *Small*, 2011, **7**, 1562-1568.
91.X. Y. Huang and J. C. Ren, *TrAC-Trends Anal. Chem.*, 2012, **40**, 77-89.
92. P. Subramanian, A. Lesniewski, I. Kaminska, A. Vlandas, A. Vasilescu, J. Niedziolka-Jonsson, E. Pichonat, H. Happy, R. Boukherroub and S. Szunerits, *Biosens. Bioelectron.*, 2013, **50**, 239-243.
93. N. Varghese, U. Mogera, A. Govindaraj, A. Das, P. K. Maiti, A. K. Sood and C. N. R. Rao, *Chemphyschem*, 2009, **10**, 206-210.
94. S. Panigrahi, A. Bhattacharya, S. Banerjee and D. Bhattacharyya, *J. Phys. Chem. C*, 2012, **116**, 4374-4379.
95. Y. Cho, S. K. Min, J. Yun, W. Y. Kim, A. Tkatchenko and K. S. Kim, *J. Chem. Theory Comput.*, 2013, **9**, 2090-2096.
96. M. Rosa, S. Corni and R. Di Felice, *J. Chem. Theory Comput.*, 2013, **9**, 4552-4561.
97. S. K. Min, Y. Cho, D. R. Mason, J. Y. Lee and K. S. Kim, *J. Phys. Chem. C*, 2011, **115**, 16247-16257.
98. M. L. Mayo, Z. Q. Chen and S. V. Kilina, *J Phys Chem Lett*, 2012, **3**, 2790-2797.
99. D. Umadevi and G. N. Sastry, *J Phys Chem Lett*, 2011, **2**, 1572-1576.
100. V. Kotikam, M. Fernandes and V. A. Kumar, *Phys. Chem. Chem. Phys.*, 2012, **14**, 15003-15006.
101. S. Gowtham, R. H. Scheicher, R. Ahuja, R. Pandey and S. P. Karna, *Phys. Rev. B*, 2007, **76**, 033401.
102. S. Akca, A. Foroughi, D. Frochtzwajg and H. W. C. Postma, *Plos One*, 2011, **6**, e18442.
103. J. Antony and S. Grimme, *Phys. Chem. Chem. Phys.*, 2008, **10**, 2722-2729.
104S. J. Sowerby, C. A. Cohn, W. M. Heckl and N. G. Holm, *Proc. Natl. Acad. Sci. U.S.A.*, 2001, **98**, 820-822.
105. M. Wu , R. Kempaiah , P.-J. J. Huang, V. Maheshwari, J. W. Liu, *Langmuir*, 2011, **27**, 2731–2738
106. M. Yi, S. Yang, Z. Peng, C. H. Liu, J. S. Li, W. W. Zhong, R. H. Yang, W. H. Tan, *Anal. Chem.*, 2014, 86, 12229-12235
107. H. X. Chang, L. H. Tang, Y. Wang, J. H. Jiang and J. H. Li, *Anal. Chem.*, 2010, **82**, 2341-2346.
108. L. Cui, Z. R. Chen, Z. Zhu, X. Y. Lin, X. Chen and C. J. Yang, *Anal. Chem.*, 2013, **85**, 2269-2275.

109. B. W. Liu, Z. Y. Sun, X. Zhang and J. W. Liu, *Anal. Chem.*, 2013, **85**, 7987-7993.
110. C. H. Lu, H. H. Yang, C. L. Zhu, X. Chen and G. N. Chen, *Angew. Chem. Int. Ed.*, 2009, **48**, 4785-4787.
111. L. H. Tang, D. Y. Li and J. H. Li, *Chem. Commun.*, 2013, **49**, 9971-9973.
112. A. J. Patil, J. L. Vickery, T. B. Scott and S. Mann, *Adv. Mater.*, 2009, **21**, 3159-3164.
113. M. Zheng, A. Jagota, E. D. Semke, B. A. Diner, R. S. McLean, S. R. Lustig, R. E. Richardson and N. G. Tassi, *Nat. Mater.*, 2003, **2**, 338-342.
114. S. J. He, B. Song, D. Li, C. F. Zhu, W. P. Qi, Y. Q. Wen, L. H. Wang, S. P. Song, H. P. Fang and C. H. Fan, *Adv. Funct. Mater.*, 2010, **20**, 453-459.
115. L. H. Tang, H. X. Chang, Y. Liu and J. H. Li, *Adv. Funct. Mater.*, 2012, **22**, 3083-3088.
116. M. Liu, H. M. Zhao, S. Chen, H. T. Yu and X. Quan, *Chem. Commun.*, 2012, **48**, 564-566.
117. H. Z. Lei, L. J. Mi, X. J. Zhou, J. J. Chen, J. Hu, S. W. Guo and Y. Zhang, *Nanoscale*, 2011, **3**, 3888-3892.
118. X. Zhao, *J. Phys. Chem. C*, 2011, **115**, 6181-6189.
119. L. Cui, Y. L. Song, G. L. Ke, Z. C. Guan, H. M. Zhang, Y. Lin, Y. S. Huang, Z. Zhu and C. J. Yang, *Chem. Eur. J.*, 2013, **19**, 10442-10451.
120. X. Q. Liu, F. Wang, R. Aizen, O. Yehezkeli and I. Willner, *J. Am. Chem. Soc.*, 2013, **135**, 11832-11839.
121. L. Cui, X. Y. Lin, N. H. Lin, Y. L. Song, Z. Zhu, X. Chen and C. J. Yang, *Chem. Commun.*, 2012, **48**, 194-196.
122. X.-X. He, K. Wang, W. Tan, B. Liu, X. Lin, C. He, D. Li, S. Huang and J. Li, *J. Am. Chem. Soc.*, 2003, **125**, 7168-7169.
123. Y. Wu, J. A. Phillips, H. Liu, R. Yang and W. Tan, *ACS Nano*, 2008, **2**, 2023-2028.
124. D. A. Giljohann, D. S. Seferos, P. C. Patel, J. E. Millstone, N. L. Rosi and C. A. Mirkin, *Nano Lett.*, 2007, **7**, 3818-3821.
125. H. K. Moon, C. I. Chang, D.-K. Lee and H. C. Choi, *Nano Research*, 2008, **1**, 351-360.
126. M. Zheng, A. Jagota, M. S. Strano, A. P. Santos, P. Barone, S. G. Chou, B. A. Diner, M. S. Dresselhaus, R. S. Mclean and G. B. Onoa, *Science*, 2003, **302**, 1545-1548.
127. D. A. Giljohann, D. S. Seferos, W. L. Daniel, M. D. Massich, P. C. Patel and C. A. Mirkin, *Angew. Chem. Int. Ed.*, 2010, **49**, 3280-3294.
128. D. S. Seferos, A. E. Prigodich, D. A. Giljohann, P. C. Patel and C. A. Mirkin, *Nano Lett.*, 2008, **9**, 308-311.
129. Z. W. Tang, H. Wu, J. R. Cort, G. W. Buchko, Y. Y. Zhang, Y. Y. Shao, I. A. Aksay, J. Liu and Y. H. Lin, *Small*, 2010, **6**, 1205-1209.
130.C. H. Lu, J. Li, J. J. Liu, H. H. Yang, X. Chen and G. N. Chen, *Chem. Eur. J.*, 2010, **16**, 4889-4894.
131. C. H. Lu, J. Li, X. J. Qi, X. R. Song, H. H. Yang, X. Chen and G. N. Chen, *J. Mater. Chem.*, 2011, **21**, 10915-10919.

132. C. H. Lu, C. L. Zhu, J. Li, J. J. Liu, X. Chen and H. H. Yang, *Chem. Commun.*, 2010, **46**, 3116-3118.
133. C. K. Wu, Y. M. Zhou, X. M. Miao and L. S. Ling, *Analyst*, 2011, **136**, 2106-2110.
134. Y. Wang, Z. H. Li, T. J. Weber, D. H. Hu, C. T. Lin, J. H. Li and Y. H. Lin, *Anal. Chem.*, 2013, **85**, 6775-6782.
135. S. Mogurampelly, S. Panigrahi, D. Bhattacharyya, A. K. Sood and P. K. Maiti, *J. Chem. Phys.*, 2012, **137**, 065106.
136. L. H. Tang, Y. Wang, Y. Liu and J. H. Li, *ACS Nano*, 2011, **5**, 3817-3822.
137. R. Heim and R. Y. Tsien, *Curr. Biol.*, 1996, **6**, 178-182.
138. P. R. Selvin, *Nat. Struct. Biol.*, 2000, **7**, 730-734.
139. G. W. Gordon, G. Berry, X. H. Liang, B. Levine and B. Herman, *Biophys. J.*, 1998, **74**, 2702-2713.
140. J. Balapanuru, J. X. Yang, S. Xiao, Q. L. Bao, M. Jahan, L. Polavarapu, J. Wei, Q. H. Xu and K. P. Loh, *Angew. Chem. Int. Ed.*, 2010, **49**, 6549-6553.
141. H. F. Dong, W. C. Gao, F. Yan, H. X. Ji and H. X. Ju, *Anal. Chem.*, 2010, **82**, 5511-5517.
142. R. S. Swathi and K. L. Sebastian, *J. Chem. Phys.*, 2008, **129**, 054703.
143. R. S. Swathi and K. L. Sebastian, *J. Chem. Phys.*, 2009, **130**, 233-240.
144. X. Wu, H. Liu, J. Liu, K. N. Haley, J. A. Treadway, J. P. Larson, N. Ge, F. Peale and M. P. Bruchez, *Nat. Biotechnol.*, 2003, **21**, 41-46.
145. X. Q. Liu, R. Aizen, R. Freeman, O. Yehezkeli and I. Willner, *ACS Nano*, 2012, **6**, 3553-3563.
146. Y. H. Lin, Y. Tao, F. Pu, J. S. Ren and X. G. Qu, *Adv. Funct. Mater.*, 2011, **21**, 4565-4572.
147. H. Xu, Q. Yang, F. Li, L. S. Tang, S. M. Gao, B. W. Jiang, X. C. Zhao, L. H. Wang and C. H. Fan, *Analyst*, 2013, **138**, 2678-2682.
148. L. P. Cai, R. Y. Zhan, K. Y. Pu, X. Y. Qi, H. Zhang, W. Huang and B. Liu, *Anal. Chem.*, 2011, **83**, 7849-7855.
149. H. F. Dong, J. Zhang, H. X. Ju, H. T. Lu, S. Y. Wang, S. Jin, K. H. Hao, H. W. Du and X. J. Zhang, *Anal. Chem.*, 2012, **84**, 4587-4593.
150. X. H. Tan, T. Chen, X. L. Xiong, Y. Mao, G. Z. Zhu, E. Yasun, C. M. Li, Z. Zhu and W. H. Tan, *Anal. Chem.*, 2012, **84**, 8622-8627.
151. T. Yang, Q. Guan, X. H. Guo, L. Meng, M. Du and K. Jiao, *Anal. Chem.*, 2013, **85**, 1358-1366.
152. H. Jang, Y. K. Kim, H. M. Kwon, W. S. Yeo, D. E. Kim and D. H. Min, *Angew. Chem. Int. Ed.*, 2010, **49**, 5703-5707.
153. H. Jang, S. R. Ryoo, Y. K. Kim, S. Yoon, H. Kim, S. W. Han, B. S. Choi, D. E. Kim and D. H. Min, *Angew. Chem. Int. Ed.*, 2013, **52**, 2340-2344.
154. X. Zhu, X. M. Zhou and D. Xing, *Chem. Eur. J.*, 2013, **19**, 5487-5494.
155. H. Pei, J. Li, M. Lv, J. Y. Wang, J. M. Gao, J. X. Lu, Y. P. Li, Q. Huang, J. Hu and C. H. Fan, *J. Am. Chem. Soc.*, 2012, **134**, 13843-13849.
156. C. F. Zhu, Z. Y. Zeng, H. Li, F. Li, C. H. Fan and H. Zhang, *J. Am. Chem. Soc.*, 2013, **135**, 5998-6001.

157. W. Li, J. S. Wang, J. S. Ren and X. G. Qu, *Angew. Chem. Int. Ed.*, 2013, **52**, 6726-6730.
158. Z. M. Markovic, B. Z. Ristic, K. M. Arsikin, D. G. Klisic, L. M. Harhaji-Trajkovic, B. M. Todorovic-Markovic, D. P. Kepic, T. K. Kravic-Stevovic, S. P. Jovanovic, M. M. Milenkovic, D. D. Milivojevic, V. Z. Bumbasirevic, M. D. Dramicanin and V. S. Trajkovic, *Biomaterials*, 2012, **33**, 7084-7092.
159. C. Zhao, L. Y. Feng, B. L. Xu, J. S. Ren and X. G. Qu, *Chem. Eur. J.*, 2011, **17**, 7007-7012.
160. R. Liu, D. Wu, X. Feng and K. Müllen, *J. Am. Chem. Soc.*, 2011, **133**, 15221-15223.
161. Z. Liu, J. T. Robinson, X. Sun and H. Dai, *J. Am. Chem. Soc.*, 2008, **130**, 10876-10877.
162. S. Essig, C. W. Marquardt, A. Vijayaraghavan, M. Ganzhorn, S. Dehm, F. Hennrich, F. Ou, A. A. Green, C. Sciascia, F. Bonaccorso, K. P. Bohnen, H. v. Löhneysen, M. M. Kappes, P. M. Ajayan, M. C. Hersam, A. C. Ferrari and R. Krupke, *Nano Lett.*, 2010, **10**, 1589-1594.
163. X. Sun, Z. Liu, K. Welsher, J. Robinson, A. Goodwin, S. Zaric and H. Dai, *Nano Research*, 2008, **1**, 203-212.
164. K. P. Loh, Q. Bao, G. Eda and M. Chhowalla, *Nat. Chem.*, 2010, **2**, 1015-1024.
165. F. Liu, H. D. Ha, D. J. Han and T. S. Seo, *Small*, 2013, **9**, 3410-3414.
166. X. L. Fu, T. T. Lou, Z. P. Chen, M. Lin, W. W. Feng and L. X. Chen, *ACS Appl. Mater. Inter.*, 2012, **4**, 1080-1086.
167. J. H. Jung, D. S. Cheon, F. Liu, K. B. Lee and T. S. Seo, *Angew. Chem. Int. Ed.*, 2010, **49**, 5708-5711.
168. Y. Piao, F. Liu and T. S. Seo, *Chem. Commun.*, 2011, **47**, 12149-12151.
169. Y. P. Song, M. Feng and H. B. Zhan, *Prog. Chem.*, 2012, **24**, 1665-1673.
170. L. H. Tang, Y. Wang, Y. M. Li, H. B. Feng, J. Lu and J. H. Li, *Adv. Funct. Mater.*, 2009, **19**, 2782-2789.
171. D. Chen, H. B. Feng and J. H. Li, *Chem. Rev.*, 2012, **112**, 6027-6053.
172. D. Chen, L. H. Tang and J. H. Li, *Chem. Soc. Rev.*, 2010, **39**, 3157-3180.
173. D. Chen, H. Zhang, Y. Liu and J. H. Li, *Energ. Environ. Sci.*, 2013, **6**, 1362-1387.
174. E. Paleček, Naturwissenschaften, 1958, **45**, 186-187.
175. E. Paleček, *Talanta*, 2002, **56**, 809-819.
176. E. Paleček, *Electroanal.*, 2009, **21**, 239-251.
177. M. Zhou, Y. M. Zhai and S. J. Dong, *Anal. Chem.*, 2009, **81**, 5603-5613.
178. L. Wu, J. S. Wang, L. Y. Feng, J. S. Ren, W. L. Wei and X. G. Qu, *Adv. Mater.*, 2012, **24**, 2447-2452.
179. A. H. Loo, A. Bonanni and M. Pumera, *Nanoscale*, 2012, **4**, 143-147.
180. A. Bonanni, A. H. Loo and M. Pumera, *Trac-Trend Anal. Chem.*, 2012, **37**, 12-21.
181. W. Li, P. Wu, H. Zhang and C. X. Cai, *Anal. Chem.*, 2012, **84**, 7583-7590.
182. L. Lin, Y. Liu, L. H. Tang and J. H. Li, *Analyst*, 2011, **136**, 4732-4737.
183. C. X. Lim, H. Y. Hoh, P. K. Ang and K. P. Loh, *Anal. Chem.*, 2010, **82**,

7387-7393.
184. E. Dubuisson, Z. Y. Yang and K. P. Loh, *Anal. Chem.*, 2011, **83**, 2452-2460.
185. H. L. Poh, A. Bonanni and M. Pumera, *RSC Adv*, 2012, **2**, 1021-1024.
186. A. H. Loo, A. Bonanni and M. Pumera, *Electrochem. Commun.*, 2013, **28**, 83-86.
187. Y. W. Hu, K. K. Wang, Q. X. Zhang, F. H. Li, T. S. Wu and L. Niu, *Biomaterials*, 2012, **33**, 1097-1106.
188. Y. W. Hu, F. H. Li, X. X. Bai, D. Li, S. C. Hua, K. K. Wang and L. Niu, *Chem. Commun.*, 2011, **47**, 1743-1745.
189. Y. W. Hu, S. C. Hua, F. H. Li, Y. Y. Jiang, X. X. Bai, D. Li and L. Niu, *Biosens. Bioelectron.*, 2011, **26**, 4355-4361.
190. F. Uslu, S. Ingebrandt, D. Mayer, S. Böcker-Meffert, M. Odenthal, and A. Offenhäusser, *Biosens. Bioelectron.*, 2004, **19,** 1723-1731
191. N. Sun, Y. Liu, L. Qin, G. Y. Xu, D. Ham, *Proceedings of the ESSCIRC, IEEE*, 2012,14-17
192. J. M. Rothberg, W. Hinz, T. M. Rearick, J. Schultz, *et al*., *Nature*, 2011, **475**, 348-352
193. F. A. H. Karimi, M. T. Ahmadi, M. Rahmani, E. Akbari, M. J. Kiani and M. Khalid, Sci. *Adv. Mater.*, 2012, **4**, 1142-1147.
194. G. Y. Xu, J. Abbott, L. Qin, K. Y.M. Yeung, Y. Song, H. Yoon, J. Kong, D. Ham, Nature Commun., 2014, 5, 5:4866.
195. X. C. Dong, Y. M. Shi, W. Huang, P. Chen, L.-J. Li, *Adv. Mater.,* 2010, **22**, 1649–1653.
196. N. Mohanty and V. Berry, *Nano Lett.*, 2008, **8**, 4469-4476.
197. T.-Y. Chen, P. T. K. Loan, C.-L. Hsu, Y.-H. Lee, J. T.-W. Wang, K.-H. Wei, C.-T. Lin, L.-J. Li，*Biosens. Bioelectron.,* 2013, **41**, 103–109
198. G. F. Schneider and C. Dekker, *Nat. Biotechnol.*, 2012, **30**, 326-328.
199. S. K. Min, W. Y. Kim, Y. Cho and K. S. Kim, *Nat. Nanotechnol.*, 2011, **6**, 162-165.
200. P. Ball, *Nat. Mater.*, 2013, 12, 950-950.
201. D. B. Wells, M. Belkin, J. Comer and A. Aksimentiev, *Nano Lett.*, 2012, **12**, 4117-4123.
202. C. Sathe, X. Q. Zou, J. P. Leburton and K. Schulten, *ACS Nano*, 2011, **5**, 8842-8851.
203. L. J. Liang, P. Cui, Q. Wang, T. Wu, H. Agren and Y. Q. Tu, *RSC Adv.*, 2013, **3**, 2445-2453.
204. S. Garaj, S. Liu, J. A. Golovchenko and D. Branton, *P. Natl. Acad. Sci. U. S. A.*, 2013, **110**, 12192-12196.
205. Z. S. Siwy and M. Davenport, *Nat. Nanotechnol.*, 2010, **5**, 697-698.
206. G. F. Schneider, S. W. Kowalczyk, V. E. Calado, G. Pandraud, H. W. Zandbergen, L. M. K. Vandersypen and C. Dekker, *Nano Lett.*, 2010, **10**, 3163-3167.
207. H. W. C. Postma, *Nano Lett.*, 2010, **10**, 420-425.
208. C. A. Merchant, K. Healy, M. Wanunu, V. Ray, N. Peterman, J. Bartel, M. D. Fischbein, K. Venta, Z. T. Luo, A. T. C. Johnson and M. Drndić, *Nano Lett.*, 2010, **10**, 2915-2921.

209. S. Garaj, W. Hubbard, A. Reina, J. Kong, D. Branton and J. A. Golovchenko, *Nature*, 2010, **467**, 190-193.
210. B. M. Venkatesan, D. Estrada, S. Banerjee, X. Z. Jin, V. E. Dorgan, M. H. Bae, N. R. Aluru, E. Pop and R. Bashir, *ACS Nano*, 2012, **6**, 441-450.
211. D. M. Vlassarev and J. A. Golovchenko, *Biophys. J.*, 2012, **103**, 352-356.
212. Gao, L.; Lian, C. Q.; Zhou, Y.; Yan, L. R.; Li, Q.; Zhang, C. X.; Chen, L.; Chen, K. P., *Biosen. Bioelectron.,* **2014,** *60*, 22-29.
213. M. Zhang, B. C. Yin, W. H. Tan and B. C. Ye, *Biosens. Bioelectron.*, 2011, **26**, 3260-3265.
214. J. R. Zhang, W. T. Huang, W. Y. Xie, T. Wen, H. Q. Luo and N. B. Li, *Analyst*, 2012, **137**, 3300-3305.
215. M. Li, X. J. Zhou, W. Q. Ding, S. W. Guo and N. Q. Wu, *Biosens. Bioelectron.*, 2013, **41**, 889-893.
216. H. Park, S. J. Hwang and K. Kim, Electro*chem. Commun.*, 2012, **24**, 100-103.
217. Y. Zhang, H. Zhao, Z. J. Wu, Y. Xue, X. F. Zhang, Y. J. He, X. J. Li and Z. B. Yuan, *Biosens. Bioelectron.*, 2013, **48**, 180-187.
218. E. Sharon, X. Q. Liu, R. Freeman, O. Yehezkeli and I. Willner, *Electroanal.*, 2013, **25**, 851-856.
219. X. H. Zhao, R. M. Kong, X. B. Zhang, H. M. Meng, W. N. Liu, W. H. Tan, G. L. Shen and R. Q. Yu, *Anal. Chem.*, 2011, **83**, 5062-5066.
220. Y. Q. Wen, C. Peng, D. Li, L. Zhuo, S. J. He, L. H. Wang, Q. Huang, Q. H. Xu and C. H. Fan, *Chem. Commun.*, 2011, **47**, 6278-6280.
221. Y. Q. Wen, F. B. Y. Li, X. C. Dong, J. Zhang, Q. H. Xiong and P. Chen, *Adv. Healthc. Mater.*, 2013, **2**, 271-274.
222. M. Liu, H. M. Zhao, S. Chen, H. T. Yu, Y. B. Zhang and X. Quan, *Biosens. Bioelectron.*, 2011, **26**, 4111-4116.
223. M. Liu, H. M. Zhao, S. Chen, H. T. Yu, Y. B. Zhang and X. Quan, *Chem. Commun.*, 2011, **47**, 7749-7751.
224. Y. Yu, Y. Liu, S. J. Zhen and C. Z. Huang, *Chem. Commun.*, 2013, **49**, 1942-1944.
225. J. H. Huang, Q. B. Zheng, J. K. Kim and Z. G. Li, *Biosens. Bioelectron.*, 2013, **43**, 379-383
226. J. Y. Kwon, N. J. Singh, H. N. Kim, S. K. Kim, K. S. Kim and J. Y. Yoon, *J. Am. Chem. Soc.*, 2004, **126**, 8892-8893.
227. J. H. Liu, C. Y. Wang, Y. Jiang, Y. P. Hu, J. S. Li, S. Yang, Y. H. Li, R. H. Yang, W. H. Tan and C. Z. Huang, *Anal. Chem.,* 2013, **85,** 1424-1430.
228. C. H. Liu, Z. Wang, H. X. Jia and Z. P. Li, *Chem. Commun.*, 2011, **47**, 4661-4663.
229. Y. He, Z. G. Wang, H. W. Tang and D. W. Pang, *Biosens. Bioelectron.*, 2011, **29**, 76-81.
230. H. F. Zhang, Y. J. Han, Y. J. Guo and C. Dong, *J. Mater. Chem.*, 2012, **22**, 23900-23905.
231. S. J. Guo, Y. Du, X. Yang, S. J. Dong and E. K. Wang, *Anal. Chem.*, 2011, **83**, 8035-8040.

232. B. Y. Jiang, M. Wang, Y. Chen, J. Q. Xie and Y. Xiang, *Biosens. Bioelectron.*, 2012, **32**, 305-308.
233. C. H. Lu, J. A. Li, M. H. Lin, Y. W. Wang, H. H. Yang, X. Chen and G. N. Chen, *Angew. Chem. Int. Ed.*, 2010, **49**, 8454-8457.
234. Y. Shi, H. C. Dai, Y. J. Sun, J. T. Hu, P. J. Ni and Z. Li, *Analyst*, 2013, **138**, 7152-7156.
235. D. P. Tang, J. Tang, Q. F. Li, B. L. Su and G. N. Chen, *Anal. Chem.*, 2011, **83**, 7255-7259.
236. P. Zhang, Y. Wang, F. Leng, Z. H. Xiong and C. Z. Huang, *Talanta*, 2013, **112**, 117-122.
237. Y. Du, S. J. Guo, H. X. Qin, S. J. Dong and E. K. Wang, *Chem. Commun.*, 2012, **48**, 799-801.
238. S. J. Wu, N. Duan, X. Y. Ma, Y. Xia, H. G. Wang, Z. P. Wang and Q. Zhang, *Anal. Chem.*, 2012, **84**, 6263-6270.
239. L. F. Sheng, J. T. Ren, Y. Q. Miao, J. H. Wang and E. K. Wang, *Biosens. Bioelectron.*, 2011, **26**, 3494-3499.
240. Y. Shi, J. Z. Wu, Y. J. Sun, Y. Zhang, Z. W. Wen, H. C. Dai, H. D. Wang and Z. Li, *Biosens. Bioelectron.*, 2012, **38**, 31-36.
241. W. Y. Xie, W. T. Huang, N. B. Li and H. Q. Luo, *Chem. Commun.*, 2012, **48**, 82-84.
242. X. Chen, Y. R. Chen, X. D. Zhou and J. M. Hu, *Talanta*, 2013, **107**, 277-283.
243. H. L. Liu, Y. H. Wang, A. G. Shen, X. D. Zhou and J. M. Hu, *Talanta*, 2012, **93**, 330-335.
244. H. Zhang, Y. Li and X. G. Su, *Anal. Biochem.*, 2013, **442**, 172-177.
245. J. H. Chen and L. W. Zeng, *Biosens. Bioelectron.*, 2013, **42**, 93-99.
246. X. M. Li, J. Song, Y. Wang and T. Cheng, *Anal. Chim. Acta*, 2013, **797**, 95-101.
247. F. Li, Y. Feng, C. Zhao, P. Li and B. Tang, *Chem. Commun.*, 2012, **48**, 127-129.
248. S. Liu, X. R. Xing, J. H. Yu, W. J. Lian, J. Li, M. Cui and J. D. Huang, *Biosens. Bioelectron.*, 2012, **36**, 186-191.
249. J. B. Zheng, Y. P. He, Q. L. Sheng and H. F. Zhang, *J. Mater. Chem.*, 2011, **21**, 12873-12879.
250. J. F. Liang, Z. B. Chen, L. Guo and L. D. Li, *Chem. Commun.*, 2011, **47**, 5476-5478.
251. Y. P. Wang, Y. H. Xiao, X. L. Ma, N. Lia and X. D. Yang, *Chem. Commun.*, 2012, **48**, 738-740.
252. Z. Zhang, L. Q. Luo, L. M. Zhu, Y. P. Ding, D. M. Deng and Z. X. Wang, Analyst, 2013, **138**, 5365-5370.
253. Y. J. Guo, Y. J. Han, Y. X. Guo and C. Dong, *Biosens. Bioelectron.*, 2013, **45**, 95-101.
254. L. J. Bai, B. Yan, Y. Q. Chai, R. Yuan, Y. L. Yuan, S. B. Xie, L. P. Jiang and Y. He, *Analyst*, 2013, **138**, 6595-6599.326-71
255. X. Y. Wang, A. Gao, C. C. Lu, X. W. He and X. B. Yin, *Biosens. Bioelectron.*, 2013, **48**, 120-125
256. L. J. Bai, R. Yuan, Y. Q. Chai, Y. L. Yuan, Y. Wang and S. B. Xie, *Chem.*

Commun., 2012, **48**, 10972-10974.
257. Y. Wang, R. Yuan, Y. Q. Chai, Y. L. Yuan and L. J. Bai, *Biosens. Bioelectron.*, 2012, **38**, 50-54.
258. Y. Wang, R. Yuan, Y. Q. Chai, Y. L. Yuan, L. J. Bai and Y. H. Liao, *Biosens. Bioelectron.*, 2011, **30**, 61-66.
259. S. B. Xie, Y. Q. Chai, R. Yuan, L. J. Bai, Y. L. Yuan and Y. Wang, *Anal. Chim. Acta*, 2012, **755**, 46-53.329-69263
260. W. Li, L. Feng, J. S. Ren, L. Wu and X. G. Qu, *Chem. Eur. J.*, 2012, **18**, 12637-12642.
261. Y. J. Guo, L. Deng, J. Li, S. J. Guo, E. K. Wang and S. J. Dong, *ACS Nano.*, 2011, **5**, 1282-1290.
262. J. Xu, J. Wu, C. Zong, H. X. Ju and F. Yan, *Anal. Chem.*, 2013, **85**, 3374-3379.
263. S. Bi, T. T. Zhao and B. Y. Luo, *Chem. Commun.*, 2012, **48**, 106-108.
264. Y. Peng, L. D. Li, X. J. Mu and L. Guo, Sensor Actuat B-chem, 2013, **177**, 818-825.
265. K. Furukawa, Y. Ueno, E. Tamechika and H. Hibino, *J. Mat. Chem. B*, 2013, **1**, 1119-1124.
266. L. Wang, C. Z. Zhu, L. Han, L. H. Jin, M. Zhou and S. J. Dong, *Chem. Commun.*, 2011, **47**, 7794-7796.
267. S. K. Bhunia and N. R. Jana, *ACS Appl. Mater. Inter.*, 2011, **3**, 3335-3341.
268. Y. H. Xiao, Y. P. Wang, M. Wu, X. L. Ma and X. D. Yang, J Electroanal Chem, 2013, **702**, 49-55.
269. G. Saltzgaber, P. Wojcik, T. Sharf, M. R. Leyden, J. L. Wardini, C. A. Heist, A. A. Adenuga, V. T. Remcho and E. D. Minot, *Nanotechnology*, 2013, **24**, 355502.
270. O. S. Kwon, S. J. Park, J. Y. Hong, A. R. Han, J. S. Lee, J. S. Lee, J. H. Oh and J. Jang, *ACS Nano*, 2012, **6**, 1486-1493.
271. Y. Ohno, K. Maehashi and K. Matsumoto, *J. Am. Chem. Soc.*, 2010, **132**, 18012-18013.
272. B. G. Choi, H. Park, M. H. Yang, Y. M. Jung, S. Y. Lee, W. H. Hong and T. J. Park, *Nanoscale*, 2010, **2**, 2692-2697.
273. K. Jayakumar, R. Rajesh, V. Dharuman, R. Venkatasan, J. H. Hahn and S. K. Pandian, *Biosens. Bioelectron.*, 2012, **31**, 406-412.
274. L. Q. Luo, Z. Zhang, Y. P. Ding, D. M. Deng, X. L. Zhu and Z. X. Wang, *Nanoscale*, 2013, **5**, 5833-5840.
275. Y. Chen, B. Y. Jiang, Y. Xiang, Y. Q. Chai and R. Yuan, *Chem. Commun.*, 2011, **47**, 12798-12800.
276. T. Yang, Q. H. Li, L. Meng, X. H. Wang, W. W. Chen and K. Jiao, *ACS Appl. Mater. Inter.*, 2013, **5**, 3495-3499.
277. Y. W. Hu, F. H. Li, D. X. Han, T. S. Wu, Q. X. Zhang, L. Niu and Y. Bao, *Anal. Chim. Acta*, 2012, **753**, 82-89.
278. D. X. Du, S. Guo, L. N. Tang, Y. Ning, Q. F. Yao and G. J. Zhang, *Sensor Actuat B-Chem*, 2013, **186**, 563-570.
279. W. Sun, Y. Y. Zhang, X. M. Ju, G. J. Li, H. W. Gao and Z. F. Sun, *Anal. Chim. Acta*, 2012, **752**, 39-44.

280. W. Sun, Y. Y. Zhang, A. H. Hu, Y. X. Lu, F. Shi, B. X. Lei and Z. F. Sun, *Electroanal.*, 2013, **25**, 1417-1424.
281. H. W. Gao, M. Sun, C. Lin and S. B. Wang, *Electroanal.*, 2012, **24**, 2283-2290.
282. Y. Z. Zhang and W. Jiang, *Electrochim. Acta*, 2012, **71**, 239-245.
283. A. Bonanni and M. Pumera, *ACS Nano*, 2011, **5**, 2356-2361.
284. H. F. Dong, Z. Zhu, H. X. Ju and F. Yan, *Biosens. Bioelectron.*, 2012, **33**, 228-232.
285. Y. Du, S. J. Guo, S. J. Dong and E. K. Wang, *Biomaterials*, 2011, **32**, 8584-8592.
286. W. L. Sun, S. Shi and T. M. Yao, *Anal. Methods*, 2011, **3**, 2472-2474.
287. S. Nandi, P. Routh, R. K. Layek and A. K. Nandi, *Biomacromolecules*, 2012, **13**, 3181-3188.
288. X. J. Xing, X. G. Liu, Y. He, Y. Lin, C. L. Zhang, H. W. Tang and D. W. Pang, *Biomacromolecules*, 2013, **14**, 117-123.
289. X. Wang, S. H. Zhong, Y. He and G. W. Song, *Anal. Methods*, 2012, **4**, 360-362.
290. S. Guo, D. X. Du, L. N. Tang, Y. Ning, Q. F. Yao and G. J. Zhang, *Analyst*, 2013, **138**, 3216-3220.
291. Y. Tao, Y. H. Lin, Z. Z. Huang, J. S. Ren and X. G. Qu, *Analyst*, 2012, **137**, 2588-2592.
292. Q. Zhu, D. S. Xiang, C. L. Zhang, X. H. Ji and Z. K. He, *Analyst*, 2013, **138**, 5194-5196
293. Balcioglu, M.; Rana, M.; Robertson, N.; Yigit, M. V. Acs Applied Materials & Interfaces 2014, 6, 12100.
294. L. Peng, Z. Zhu, Y. Chen, D. Han and W. H. Tan, *Biosens. Bioelectron.*, 2012, **35**, 475-478.
295. T. Miyahata, Y. Kitamura, A. Futamura, H. Matsuura, K. Hatakeyama, M. Koinuma, Y. Matsumoto and T. Ihara, *Chem. Commun.*, 2013, **49**, 10139-10141.
296. Z. Li, W. P. Zhu, J. W. Zhang, J. H. Jiang, G. L. Shen and R. Q. Yu, *Analyst*, 2013, **138**, 3616-3620.
297. A. Cerf, T. Alava, R. A. Barton and H. G. Craighead, *Nano Lett.*, 2011, **11**, 4232-4238.
298. M. Luo, X. Chen, G. H. Zhou, X. Xiang, L. Chen, X. H. Ji and Z. K. He, *Chem. Commun.*, 2012, **48**, 1126-1128.
299. C. Chen and B. X. Li, *J. Mater. Chem. B*, 2013, **1**, 2476-2481.
300. H. Jeong, H. S. Kim, S. H. Lee, D. Lee, Y. H. Kim and N. Huh, *Appl. Phys. Lett.*, 2013, **103**, 023701.
301. A. Girdhar, C. Sathe, K. Schulten and J. P. Leburton, *Proc. Natl. Acad. Sci. U.S.A.*, 2013, **110**, 16748-16753.
302. C. Hyun, H. Kaur, R. Rollings, M. Xiao and J. L. Li, *ACS Nano*, 2013, **7**, 5892-5900.
303. L. A. L. Tang, J. Z. Wang and K. P. Loh, *J. Am. Chem. Soc.*, 2010, **132**, 10976-10977.
304. M. Du, T. Yang and K. Jiao, *J. Mater. Chem.*, 2010, **20**, 9253-9260.
305. X. C. Dong, Y. M. Shi, W. Huang, P. Chen and L. J. Li, *Adv. Mater.*, 2010, **22**, 1649-1653.

306. A. Bonanni, C. K. Chua, G. J. Zhao, Z. Sofer and M. Pumera, *ACS Nano*, 2012, **6**, 8546-8551.
307. M. Liu, H. M. Zhao, S. Chen, H. T. Yu, Y. B. Zhang and X. Quan, *Biosens. Bioelectron.*, 2011, **26**, 4213-4216.
308. J. Li, Y. Huang, D. F. Wang, B. Song, Z. H. Li, S. P. Song, L. H. Wang, B. W. Jiang, X. C. Zhao, J. Yan, R. Liu, D. N. He and C. H. Fan, *Chem. Commun.*, 2013, **49**, 3125-3127.
309. A. N. Sidorov and T. M. Orlando, *J. Phys. Chem. Lett.*, 2013, **4**, 2328-2333.
310. D. M. Zhou, Q. Xi, M. F. Liang, C. H. Chen, L. J. Tang and J. H. Jiang, *Biosens. Bioelectron.*, 2013, **41**, 359-365.
311. J. Lee, Y. K. Kim and D. H. Min, *Anal. Chem.*, 2011, **83**, 8906-8912.
312. Y. Q. Tu, W. Li, P. Wu, H. Zhang and C. X. Cai, *Anal. Chem.*, 2013, **85**, 2536-2542.
313. L. Yang, C. H. Liu, W. Ren and Z. P. Li, *ACS Appl. Mate. Inter.*, 2012, **4**, 6450-6453.
314. H. S. Yin, Y. L. Zhou, H. X. Zhang, X. M. Meng and S. Y. Ai, *Biosens. Bioelectron.*, 2012, **33**, 247-253.
315. R. Hernandez, C. Valles, A. M. Benito, W. K. Maser, F. X. Rius and J. Riu, *Biosens. Bioelectron.*, 2014, **54**, 553-557.
316. Y. F. Duan, Y. Ning, Y. Song and L. Deng, *Microchim. Acta*, 2014, **181**, 647-653.
317. A. Singh, G. Sinsinbar, M. Choudhary, V. Kumar, R. Pasricha, H. N. Verma, S. P. Singh and K. Arora, *Sensor Actuat B-Chem*, 2013, **185**, 675-684
318. P. Zuo, X. J. Li, D. C. Dominguez and B. C. Ye, *Lab Chip*, 2013, **13**, 3921-3928.
319. L. Y. Feng, Y. Chen, J. S. Ren and X. G. Qu, *Biomaterials*, 2011, **32**, 2930-2937.
320. M. Yan, G. Q. Sun, F. Liu, J. J. Lu, J. H. Yu and X. R. Song, *Anal. Chim. Acta*, 2013, **798**, 33-39.
321. Y. Tao, Y. H. Lin, Z. Z. Huang, J. S. Ren and X. G. Qu, *Adv. Mater.*, 2013, **25**, 2594-2599.
322. G. F. Jie, Y. B. Zhao and S. Y. Niu, *Biosens. Bioelectron.*, 2013, **50**, 368-372.
S. Y. Deng and H. X. Ju, *Analyst*, 2013, **138**, 43-61.
323. W. Wei, D. F. Li, X. H. Pan and S. Q. Liu, *Analyst*, 2012, **137**, 2101-2106.
324. L. L. Cao, L. W. Cheng, Z. Y. Zhang, Y. Wang, X. X. Zhang, H. Chen, B. H. Liu, S. Zhang and J. L. Kong, *Lab Chip*, 2012, **12**, 4864-4869.
325. H. J. Li, F. Y. Liu, S. G. Sun, J. Y. Wang, Z. Y. Li, D. Z. Mu, B. Qiao and X. J. Peng, *J. Mater. Chem. B*, 2013, **1**, 4146-4151.
326. S. R. Ryoo, J. Lee, J. Yeo, H. K. Na, Y. K. Kim, H. Jang, J. H. Lee, S. W. Han, Y. Lee, V. N. Kim and D. H. Min, *ACS Nano*, 2013, 7, 5882-5891.
327. C. L. Guo, B. Book-Newell and J. Irudayaraj, *Chem. Commun.*, 2011, **47**, 12658-12660.
328. H. B. Wang, Q. Zhang, X. Chu, T. T. Chen, J. Ge and R. Q. Yu, *Angew. Chem. Int. Ed.*, 2011, **50**, 7065-7069.
329. L. Z. Feng, X. Z. Yang, X. Z. Shi, X. F. Tan, R. Peng, J. Wang and Z. Liu, *Small*, 2013, **9**, 1989-1997.
330. B. A. Chen, M. Liu, L. M. Zhang, J. Huang, J. L. Yao and Z. J. Zhang, *J. Mater.*

Chem., 2011, **21**, 7736-7741.
331. L. Z. Feng, S. A. Zhang and Z. A. Liu, *Nanoscale*, 2011, **3**, 1252-1257.
332. H. F. Dong, L. Ding, F. Yan, H. X. Ji and H. X. Ju, *Biomaterials*, 2011, **32**, 3875-3882.
333. T. B. Ren, L. Li, X. J. Cai, H. Q. Dong, S. M. Liu and Y. Y. Li, *Polym. Chem.*, 2012, **3**, 2561-2569.
334. S. Kim, S. R. Ryoo, H. K. Na, Y. K. Kim, B. S. Choi, Y. Lee, D. E. Kim and D. H. Min, *Chem. Commun.*, 2013, **49**, 8241-8243.
335. X. Zhou, F. Laroche, G. E. M. Lamers, V. Torraca, P. Voskamp, T. Lu, F. Q. Chu, H. P. Spaink, J. P. Abrahams and Z. F. Liu, *Nano Res.*, 2012, **5**, 703-709.
336. J. Y. Liu, S. J. Guo, L. Han, T. S. Wang, W. Hong, Y. Q. Liu and E. K. Wang, *J. Mater. Chem.*, 2012, **22**, 20634-20640.
337. C. Y. Wang, S. Ravi, U. S. Garapati, M. Das, M. Howell, J. Mallela, S. Alwarappan, S. S. Mohapatra and S. Mohapatra, *J. Mater. Chem. B*, 2013, **1**, 4396-4405.
338. Z. M. Markovic, L. M. Harhaji-Trajkovic, B. M. Todorovic-Markovic, D. P. Kepic, K. M. Arsikin, S. P. Jovanovic, A. C. Pantovic, M. D. Dramicanin and V. S. Trajkovic, *Biomaterials*, 2011, **32**, 1121-1129.
339. W. D. Pu, L. Zhang and C. Z. Huang, *Anal. Methods, 2012*, **4**, 166**2-**1666.
340. W. P. Zhu, Z. W. Zhao, Z. Li, J. H. Jiang, *G. L. Shen an*d R. Q. **Y**u, *Analyst*, 2012, **137**, 5506-5509.
341. D. P. Tang, J. Tang, Q. F. Li, B. Q. Liu, H. H. Yang and G. N. Chen, *RSC Adv.*, 2011, **1**, 40-43.
342. L. Wang, X. Y. Qin, S. Liu, Y. L. Luo, A. M. Asiri, A. O. Al-Youbi and X. P. Sun, *Chempluschem*, 2012, **77**, 19-22.
343. J. J. Lu, M. Yan, L. Ge, S. G. Ge, S. W. Wang, J. X. Yan and J. H. Yu, *Biosens. Bioelectron.*, 2013, **47**, 271-277.
344. L. Wang, X. Y. Qin, S. Liu, Y. L. Luo, A. M. Asiri, A. O. Al-Youbi and X. P. Sun, *Chempluschem*, 2012, **77**, 19-22.345.
345. P. J. J. Huang and J. W. Liu, *Anal. Chem.*, 2012, **84**, 4192-4198.
346. Y. Gao, Y. Li, X. Zou, H. Huang and X. G. Su, *Anal. Chim. Acta*, 2012, **731**, 68-74.
347. L. X. Zeng, A. Z. Zhang, X. H. Zhu, C. Y. Zhang, Y. Liang and J. M. Nan, *J. Electroanal. Chem.*, 2013, **703**, 153-157.
348. H. X. Qin, J. Y. Liu, C. G. Chen, J. H. Wang and E. K. Wang, *Anal. Chim. Acta*, 2012, **712**, 127-131.
349. L. P. Jiang, R. Yuan, Y. Q. Chai, Y. L. Yuan, L. J. Bai and Y. Wang, *Analyst*, 2012, **137**, 2415-2420.
350. J. R. Chen, X. X. Jiao, H. Q. Luo and N. B. Li, *J. Mater. Chem. B*, 2013, **1**, 861-864.
351. Y. L. Yuan, G. P. Liu, R. Yuan, Y. Q. Chai, X. X. Gan and L. J. Bai, *Biosens. Bioelectron.*, 2013, **42**, 474-480.
352.Y. H. Liao, R. Yuan, Y. Q. Chai, L. Mao, Y. Zhuo, Y. L. Yuan, L. J. Bai and S. R. Yuan, *Sensor Actuat B-Chem*, 2011, **158**, 393-399.

353.Y. S. Guo, X. P. Jia and S. S. Zhang, *Chem. Commun.*, 2011, **47**, 725-727.
354. F. F. Cheng, W. Chen, L. H. Hu, G. Chen, H. T. Miao, C. Z. Li and J. J. Zhu, *J. Mater. Chem. B*, 2013, **1**, 4956-4962.
355. H. Kim, R. Namgung, K. Singha, I. K. Oh and W. J. Kim, *Bioconjugate Chem.*, 2011, **22**, 2558-2567.